Responses of Global Equatorial/Low-latitude Ionosphere and Thermosphere to CME-driven and CIR-driven Geomagnetic Storms

Andrew AKALA[1] and Yuichi OTSUKA[2]

[1]University of Lagos, Lagos, Nigeria

[2]Nagoya University, Nagoya, Japan

ICELLI-SEPT-2022

Outline

1. Introduction
2. Results
3. Summary

Space Weather

Space weather is a combination of time-varying conditions of physical processes, originating from the Sun, propagating and creating disturbances along the interplanetary medium to cause impacts on the Earth's space environment.

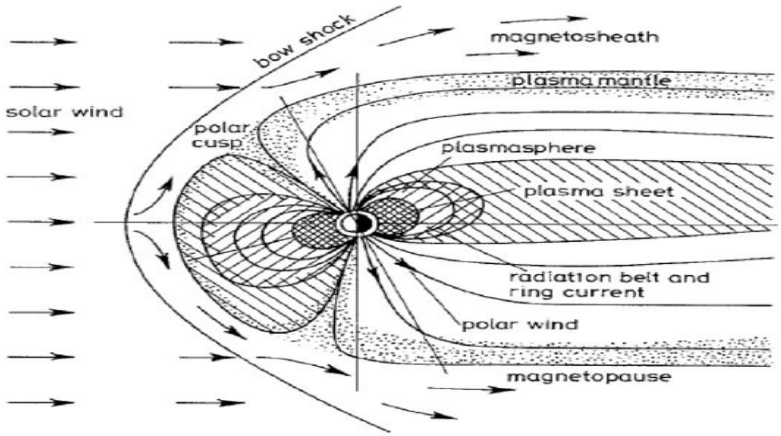

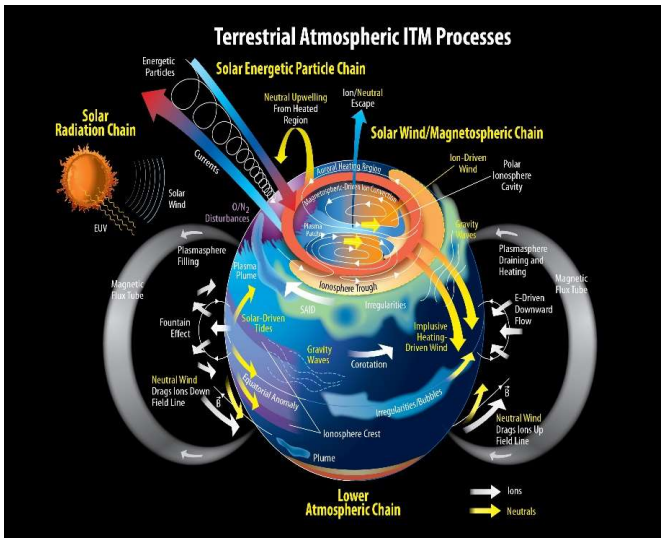

Introduction

Space Weather

Space Weather is the physical and phenomenological state of natural space environments. The associated discipline aims, through observation, monitoring, analysis and modelling, at understanding and predicting the state of the Sun, the interplanetary and planetary environments, and the solar and non-solar driven perturbations that affect them, and also at forecasting and now-casting the potential impacts on biological and technological systems. - COST Action 724 , 2009

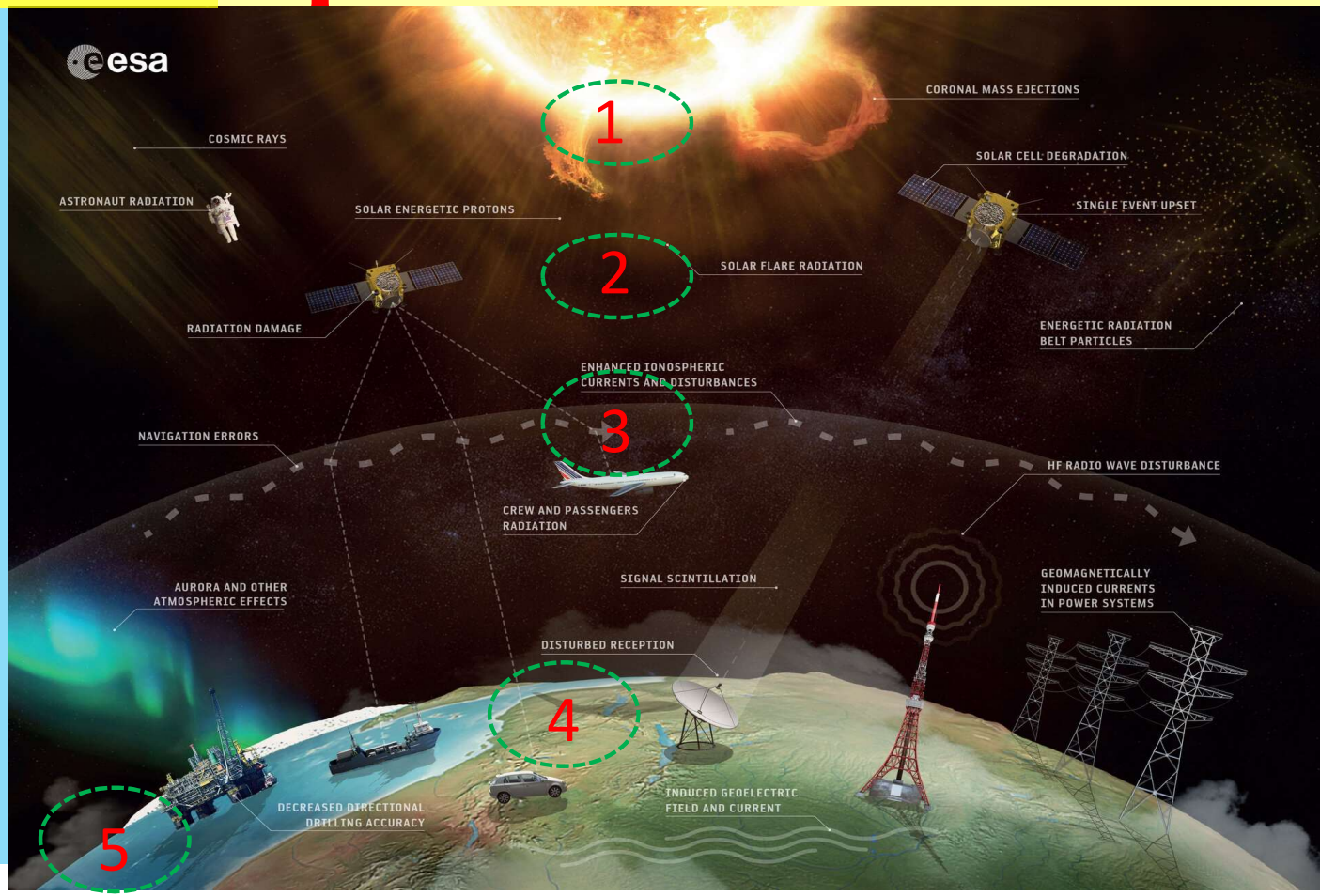

Fig. credit: ESA

https://www.esa.int/var/esa/storage/images/esa_multimedia/images/2018/01/space_weather_effects/17231521-7-eng-GB/Space_weather_effects_pillars.jpg

Motivation

Understanding of solar-magnetospheric-ionospheric coupling processes that lead to space weather events are in the front burner of the space weather community (Akala et al., 2021).

Arising from the above, space weather community is set to build prediction capabilities to preserve our common systems. The ability to quantify the impacts of past space weather events on systems is needed to accomplish this task.

Space weather components: Radio blackout; Solar Radiation Storm; **Geomagnetic Storms**; …..

Geomagnetic Storms

Geomagnetic storms are geomagnetic disturbances introduced into the geo-space by interplay of solar and interplanetary events.

The geoeffectiveness of a space weather event is the extent of geomagnetic disturbances introduced into the geo-space by interplay of solar and interplanetary events and their overall impacts on biological and technological systems (space-based and ground-based tech).

There are 2 main geoeffective heliospheric structures that cause G-storm; the ICMEs and HSS/CIR

Scope

In this study, we considered four geomagnetic storms:

(a) CME-driven geomagnetic storms:

(1) 17 March 2013
(2) 17 March 2015 } **St. Patrick's Day**

(b) CIR-driven geomagnetic storms:

(1) 1 June 2013

(2) 7 October 2015

Solar Events Precursors for the 17 March 2013 CME Storm

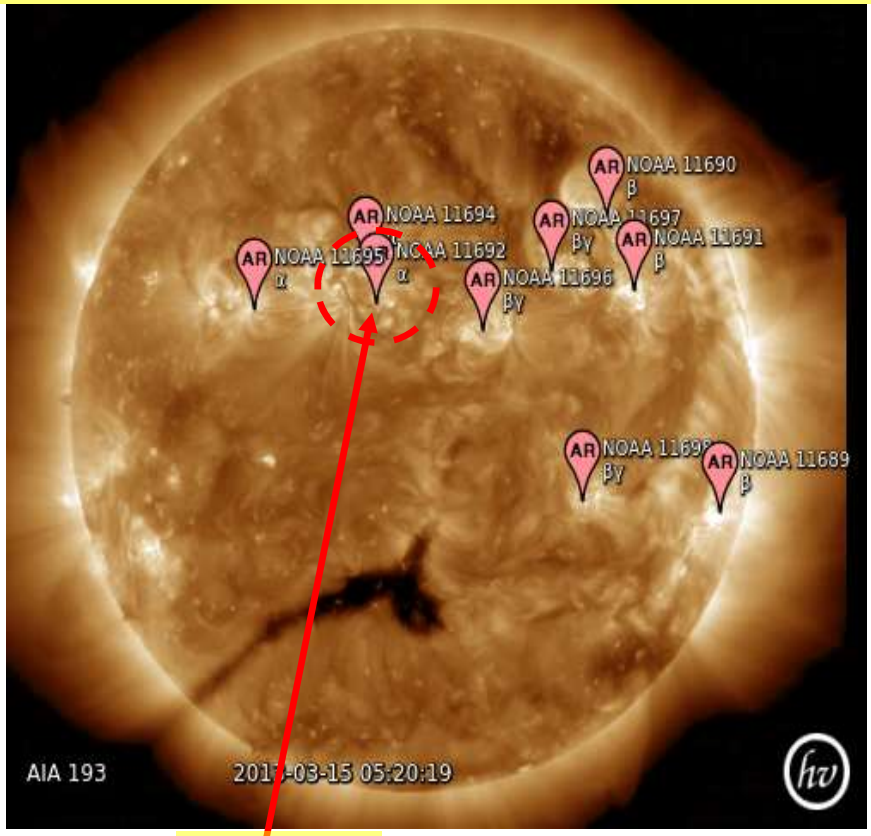

AR1692

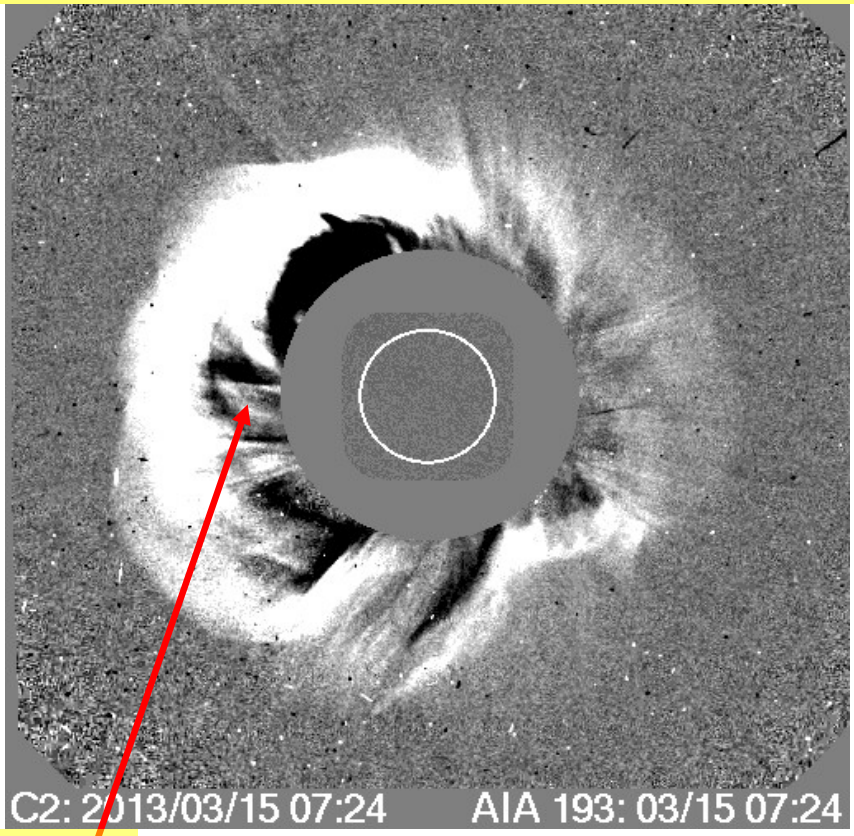

CME

Solar Events Precursors for the 17 March 2015 CME-Storm

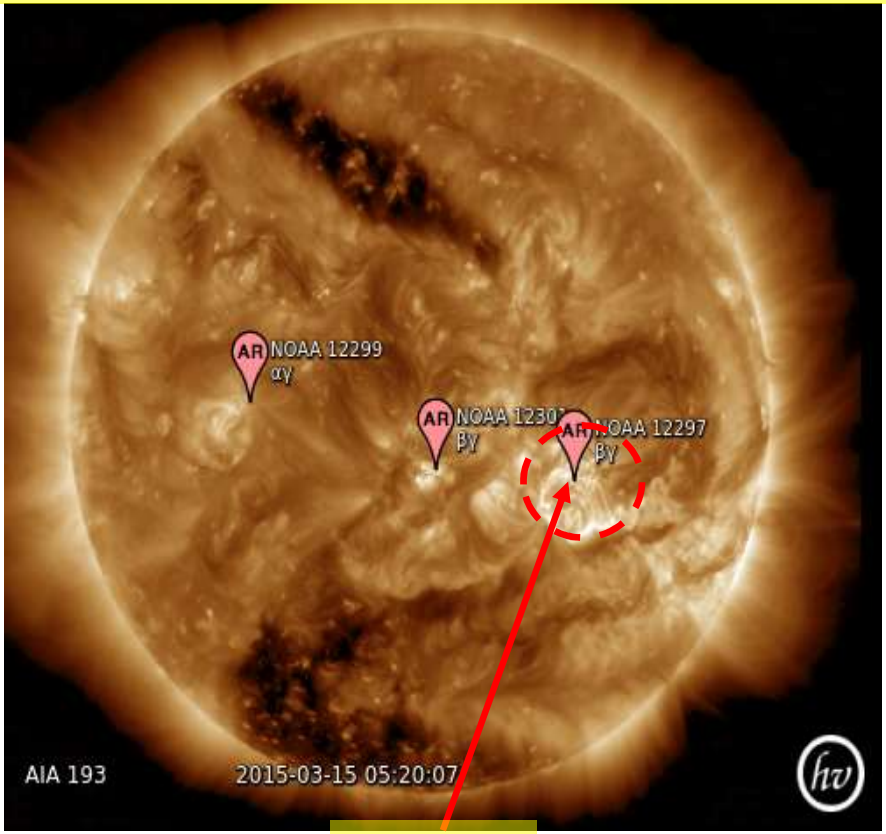

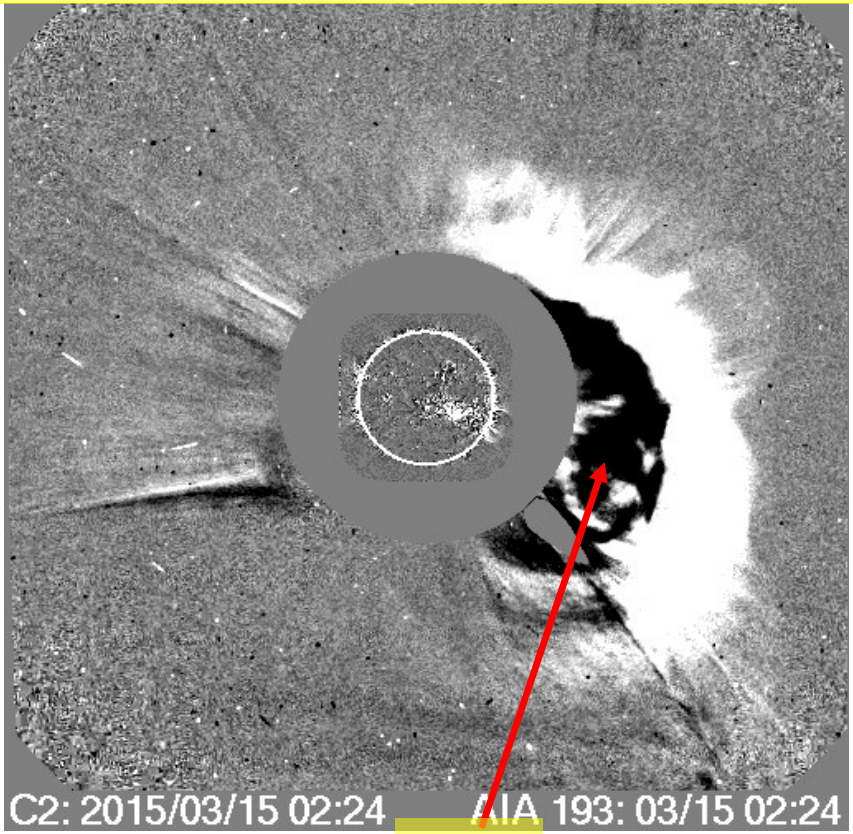

Solar Events Precursors for the 2 CIR-Storms of 1 June 2013 and 7 October 2015

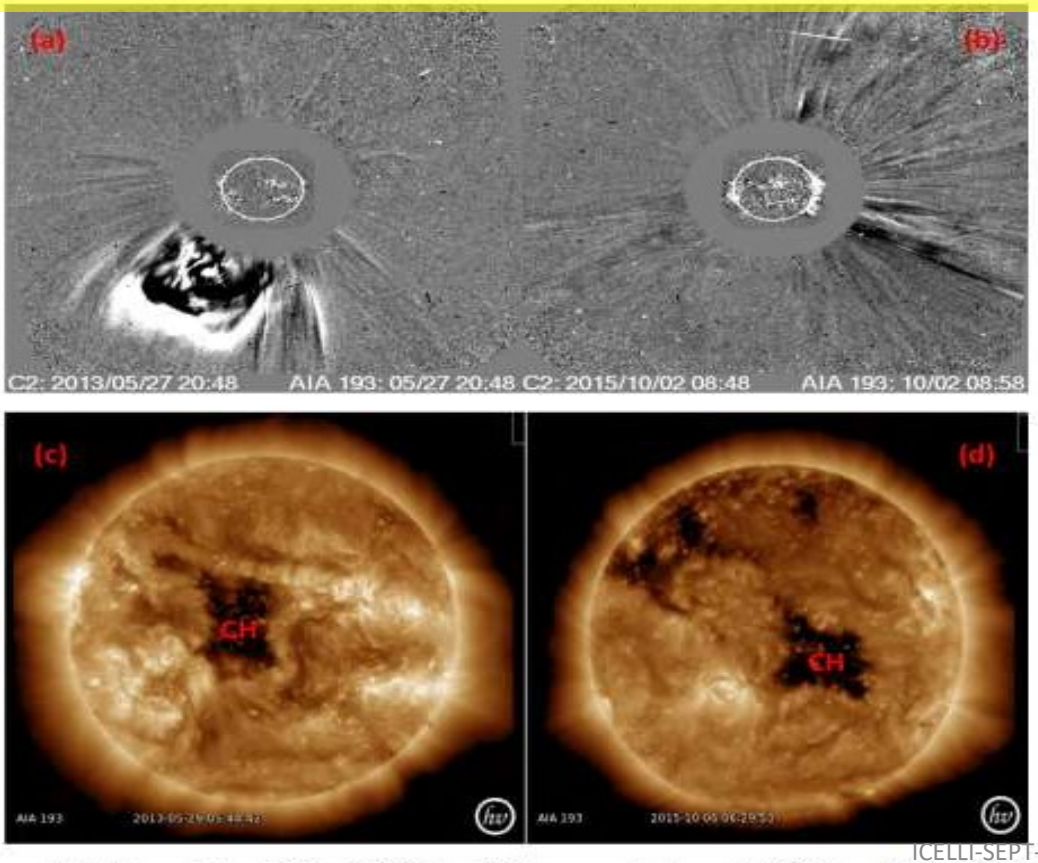

Adapted from Oyedokun et al. (2022), ASR, solar events that drove the CIR storms. (a) CME on 27 May 2013, (b) No CME on 2 October 2015, (c) Trans-equatorial Coronal Hole (CH) on 29 May 2013, (d) Trans-equatorial and solar northern hemisphere Coronal Holes (CHs) on 6 October 2015

Interplanetary Events: CME G-Storms

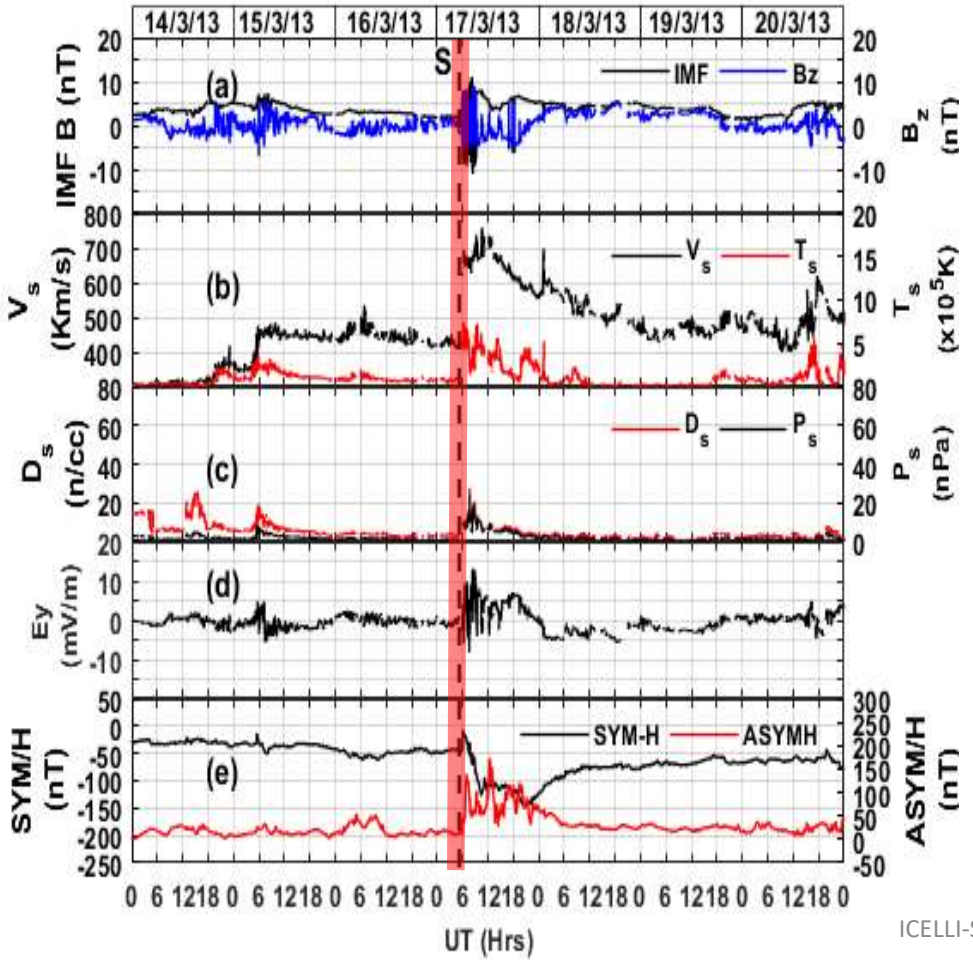

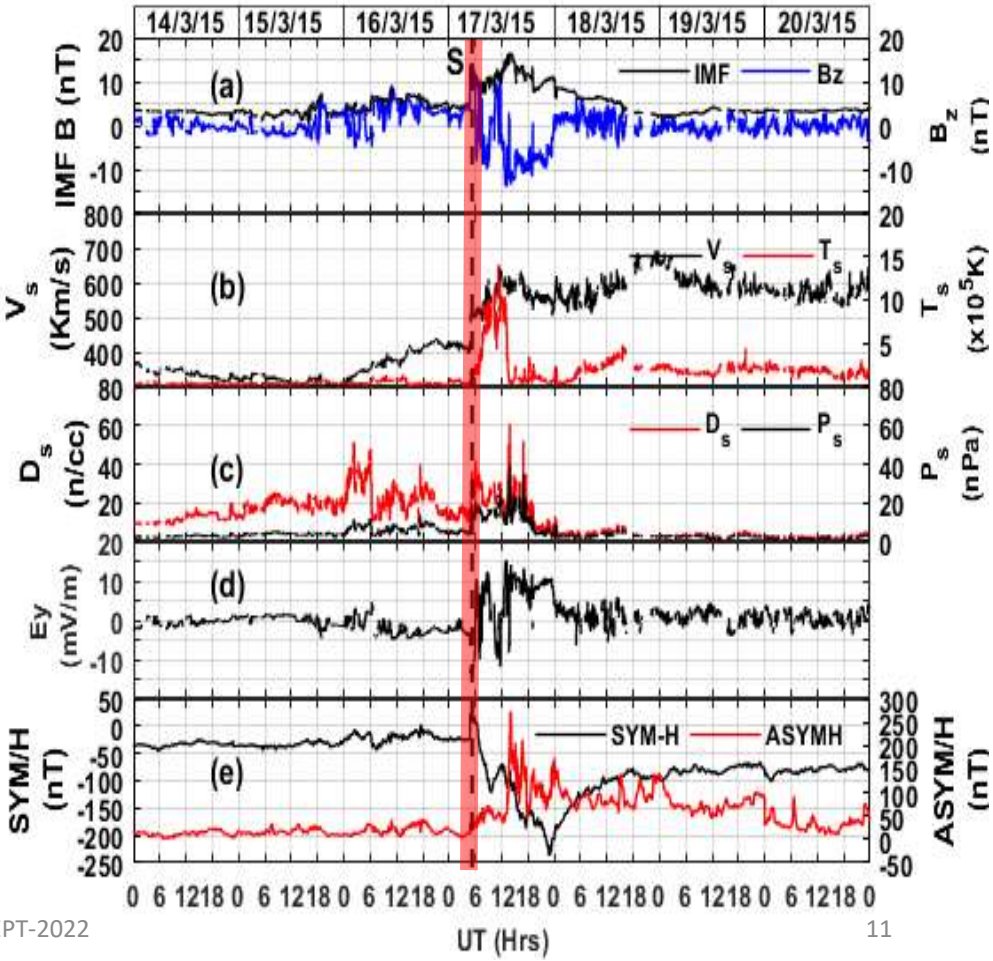

Interplanetary Events: CIR G-Storms

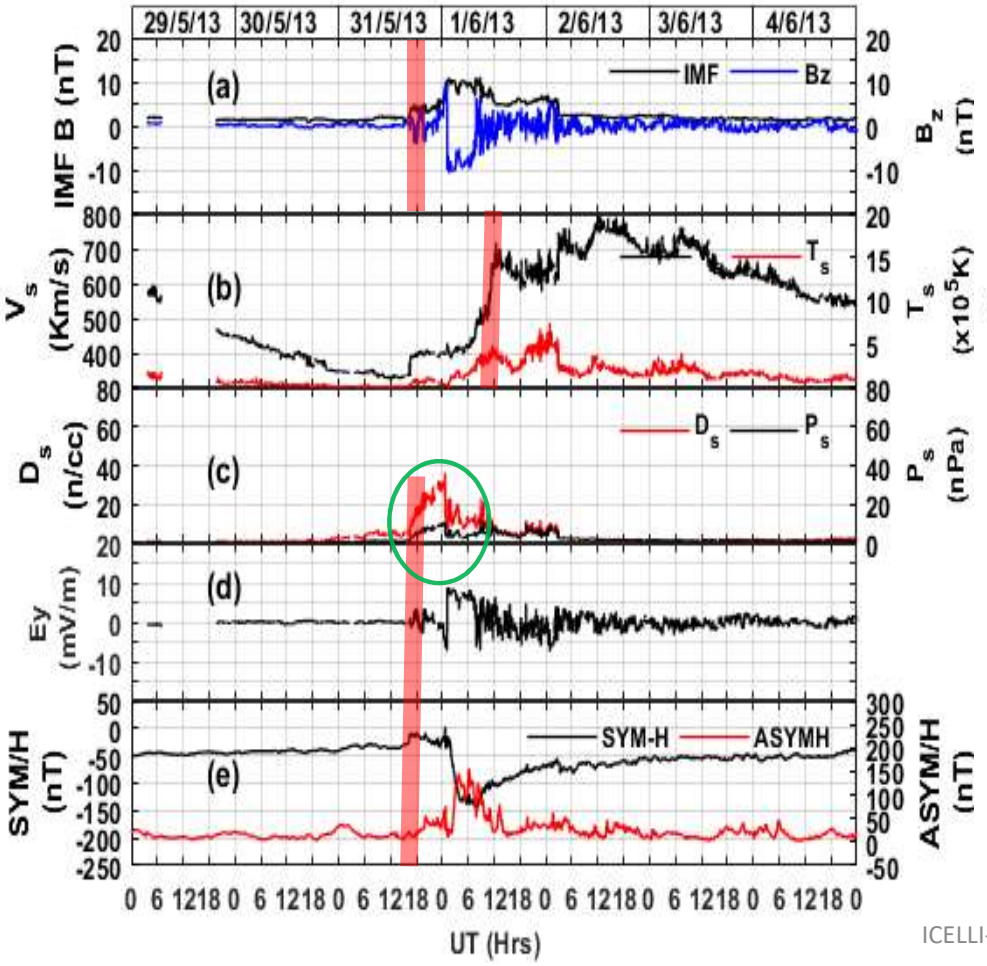

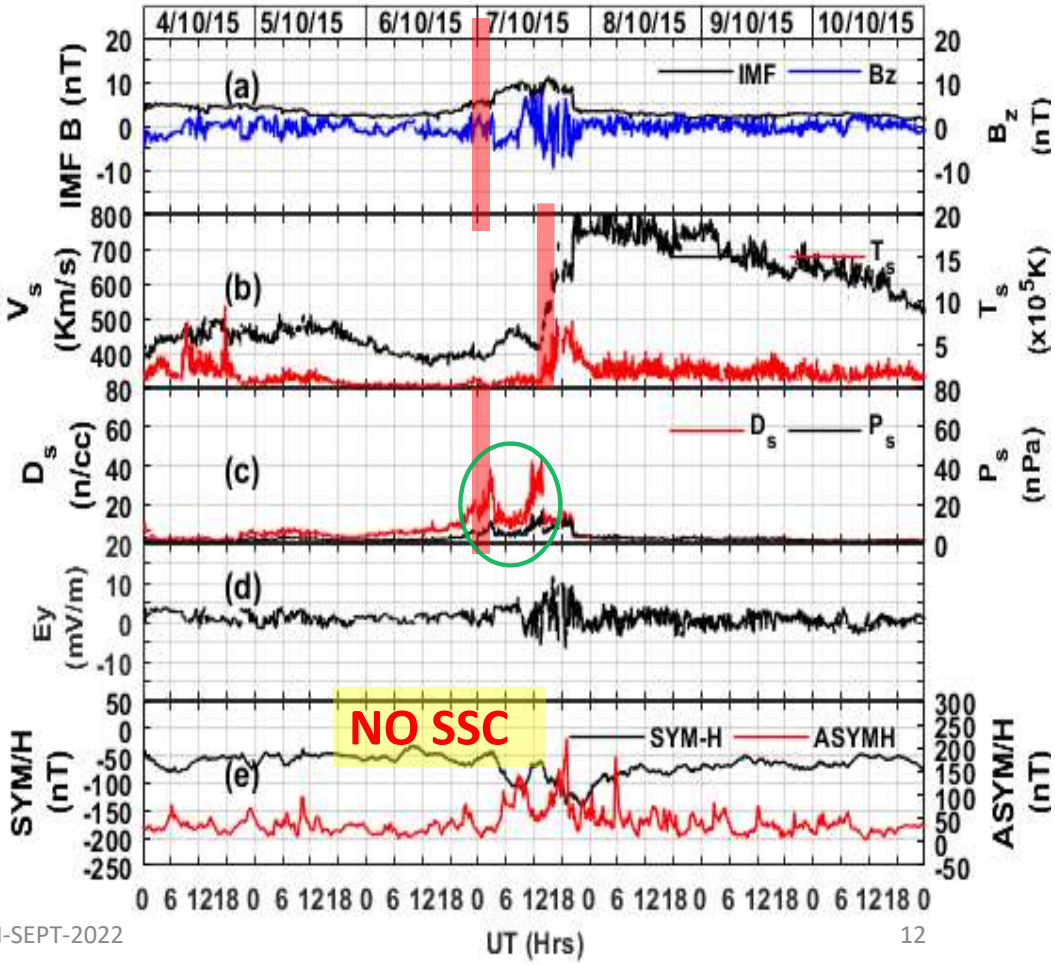

What is the extent of geoeffectiveness of these storms on global equatorial and low-latitude ionosphere?

Map showing Magnetometer and GNSS Stations

1. Pacific West
2. S/America
3. Africa
4. Indian Ocean/Asia
5. Pacific East

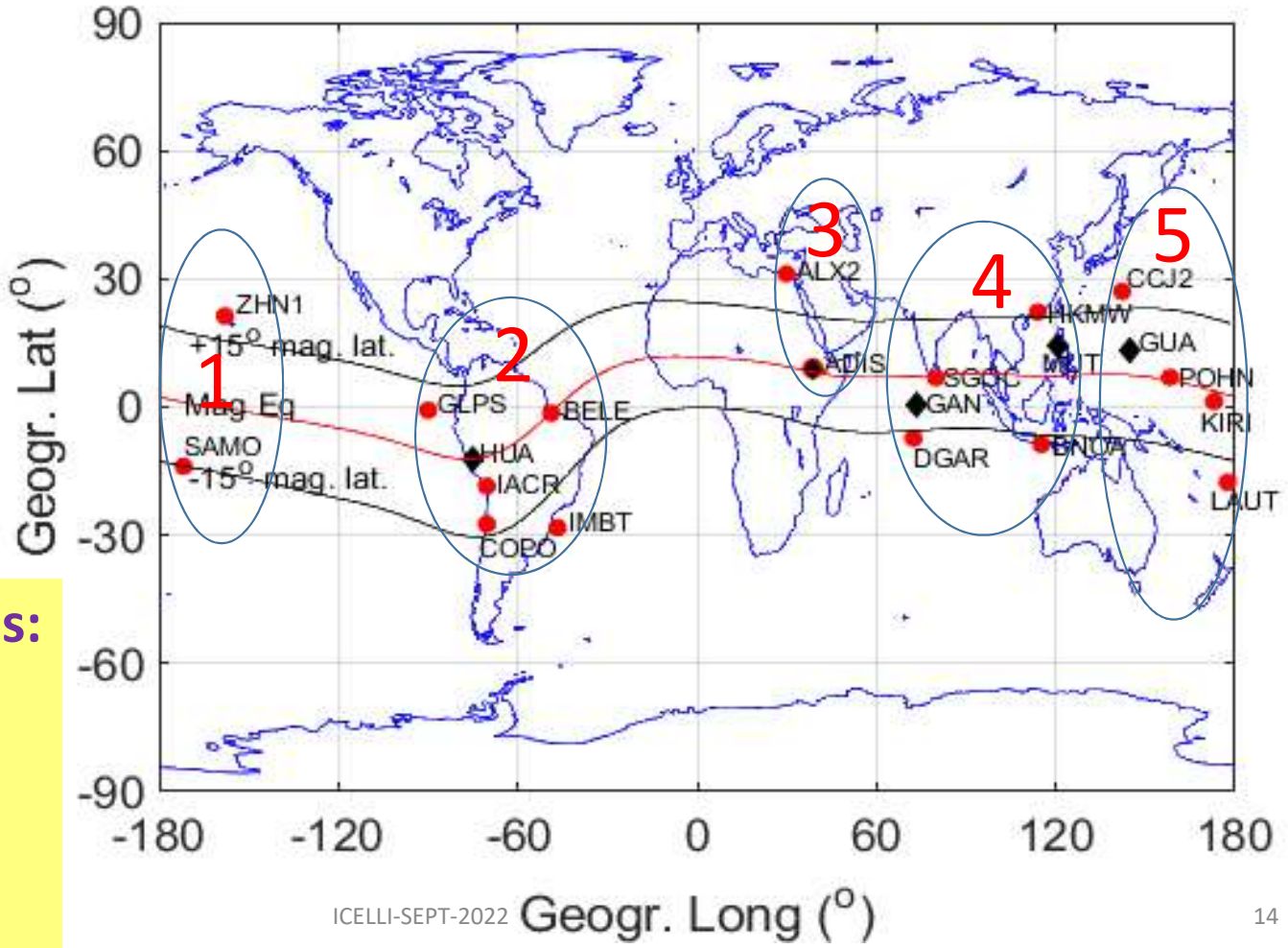

Magnetometer Stations: Black Filled Diamonds

GNSS Stations: Red Filled Circles

Table 1: GNSS Stations' Parameters

S/N	Code	City	Country	Lon. Sector	Geo. Lat	Geo. Lon	Mag. Lat	Time Zone
1	SAMO	Fagali'i	Samoa	West Pacific	-13.84	-171.73	-15.38	+13
2	ZHN1	Honolulu	USA	West Pacific	21.312	-157.92	21.67	-10
3	COPO	Copiapo	Chile	S/America	-27.38	-70.33	-14.11	-3
4	IACR	Arica	Chile	S/America	-18.47	-70.31	-5.59	-3
5	GLPS	Puerto Ayora	Ecuador	S/America	-0.74	- 90.30	9.45	-6

Table 1 Con'd

6	IMBT	Imbituba	Brazil	S/America	-28.23	-48.65	-19.74	-3
7	BELE	Belem-Para	Brazil	S/America	-1.40	-48.46	2.59	-3
8	ADIS	Addis Ababa	Ethiopia	Africa	9.03	38.76	0.18	+3
9	ALX2	Alexandria	Egypt	Africa	31.19	29.91	23.30	+2
10	DGAR	Diego Gracia	UK	Indian Ocean	-7.26	72.37	-16.88	+6
11	SGOC	Sri Lanka	Colombo	Indian Ocean	6.89	79.87	-1.57	+5.5

Table 1 Con'd

12	BNOA	Benoa	Indonesia	Asia	-8.74	115.20	-18.19	+8
13	HKMW	Lantau Island	Hong kong	Asia	22.25	114.00	15.21	+8
14	CCJ2	Ogasawara	Japan	East Pacific	27.06	142.19	19.56	+9
15	POHN	Pohn Pei	Micronesia	East Pacific	6.95	158.21	0.35	+11
16	KIRI	Betio	Kiribati	East Pacific	1.35	172.92	-2.32	+12
17	LAUT	Lautoka	Fiji	East Pacific	-17.60	177.44	-21.52	+12

Table 2: Magnetometer Stations' Parameters

S/N	Code	City	Country	Lon. Sector	Geo. Lat	Geo. Lon	Mag. Lat
1	HUA	Huancayo	PERU	S/America	-12.05	284.67	1.17
2	AAE	Addis Ababa	Ethiopia	Africa	9.03	38.77	-0.18
3	GAN	Gan	Addu Atoll	Indian Ocean	0.69	73.15	-7.77
4	MUT	Muntinlupa	Philippines	Asia	14.37	121.02	6.90
5	GUA	Guam	Guam/USA	P Ocean/W	13.59	144.87	5.64

CME G-Storms

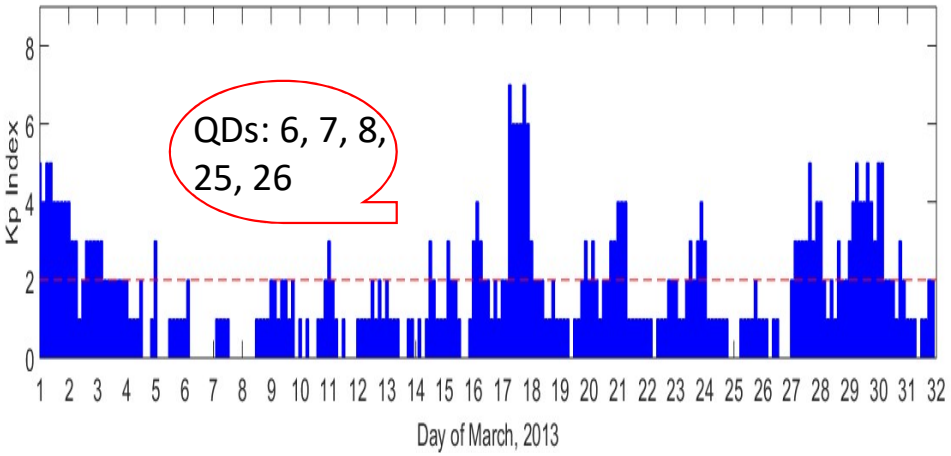

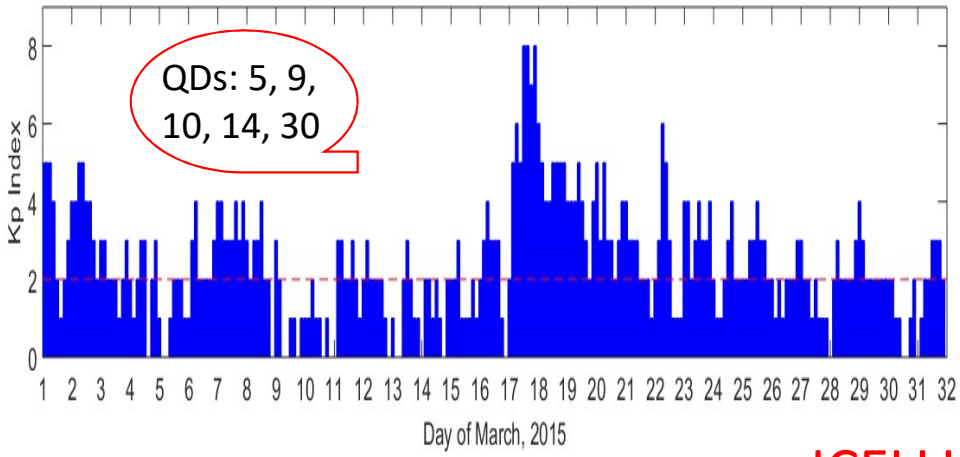

CIR G-Storms

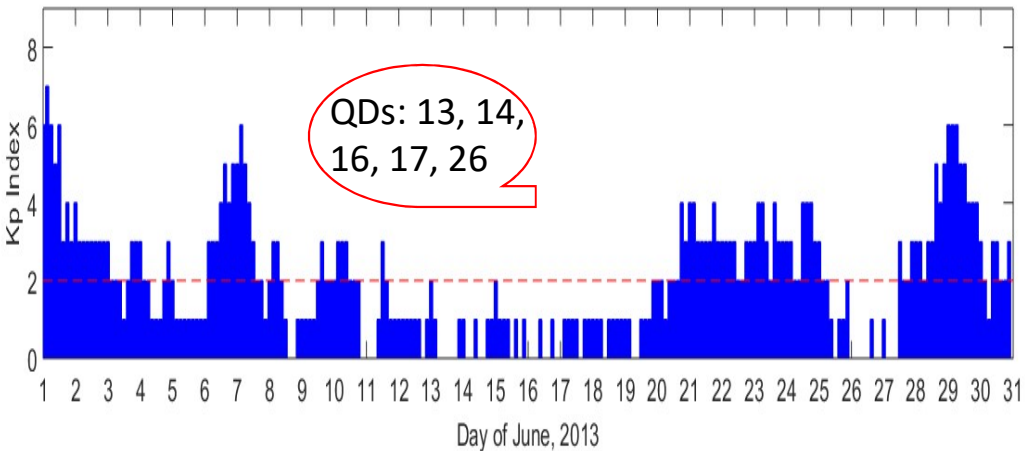

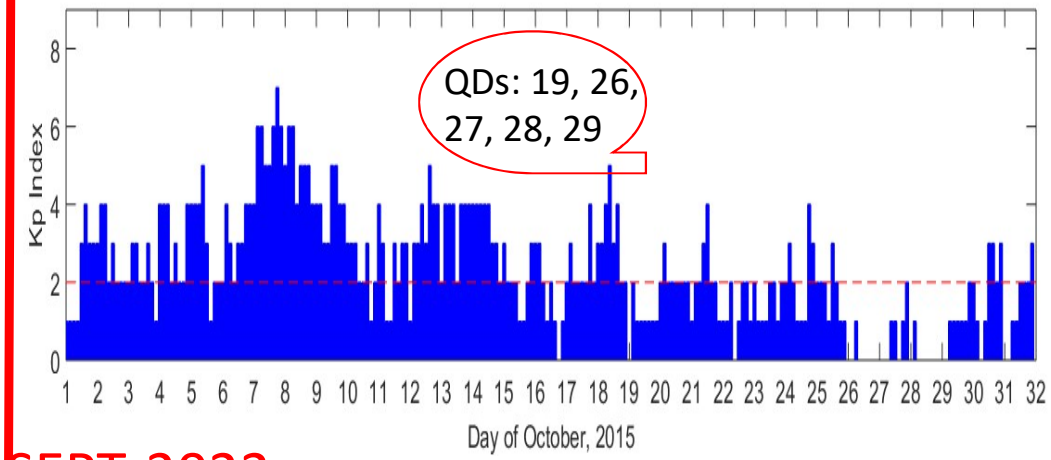

Storm 1: 17 March 2013

CME-driven geomagnetic storm

Storm 1: CME

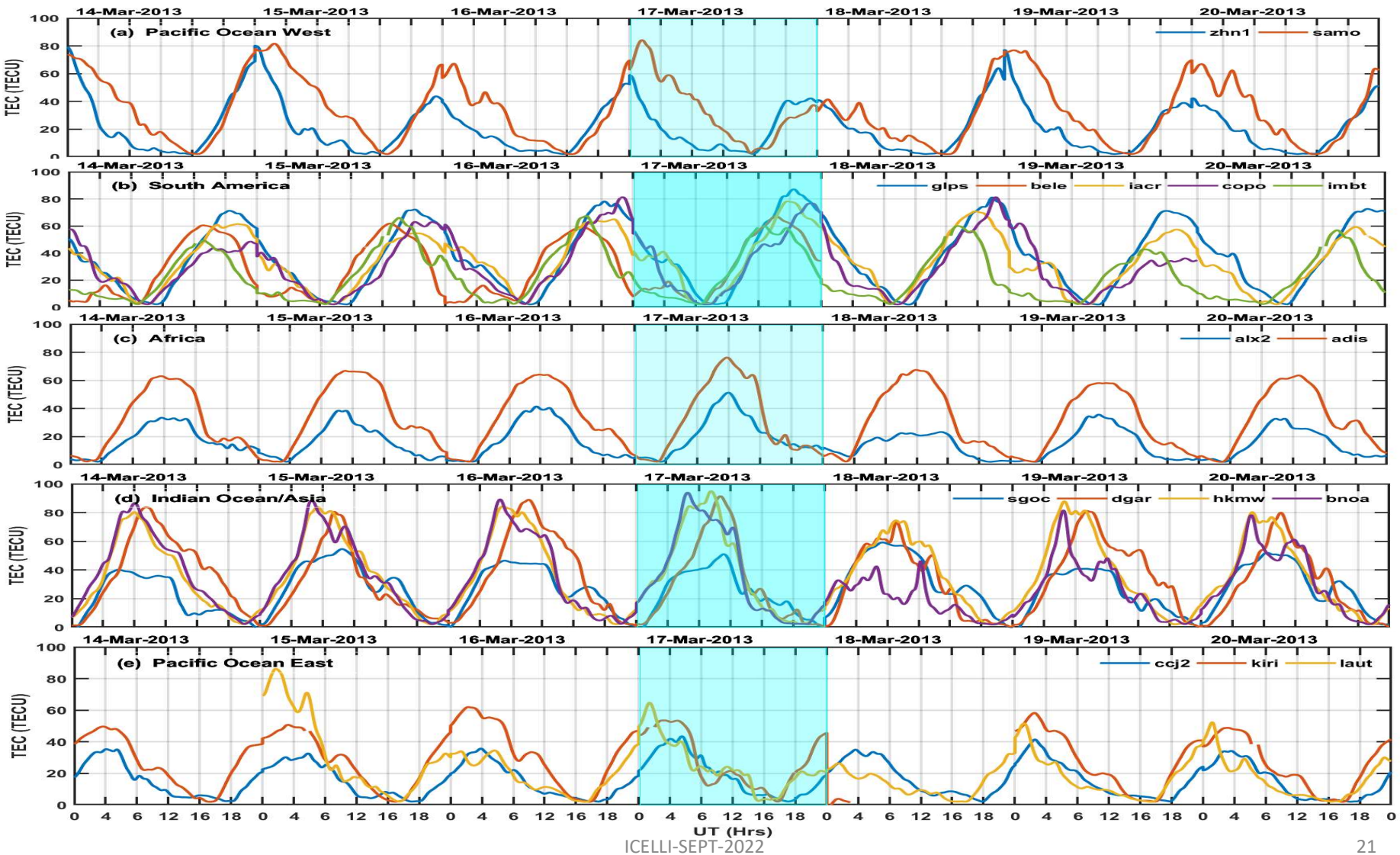
14-Mar-2013
15-Mar-2013
16-Mar-2013
17-Mar-2013
18-Mar-2013
19-Mar-2013
20-Mar-2013
(a) Pacific Ocean West
zhn1
samo
(b) South America
glps
bele
iacr
copo
imbt
(c) Africa
alx2
adis
(d) Indian Ocean/Asia
sgoc
dgar
hkmw
bnoa
(e) Pacific Ocean East
ccj2
kiri
laut
TEC (TECU)
UT (Hrs)

Storm 1: CME

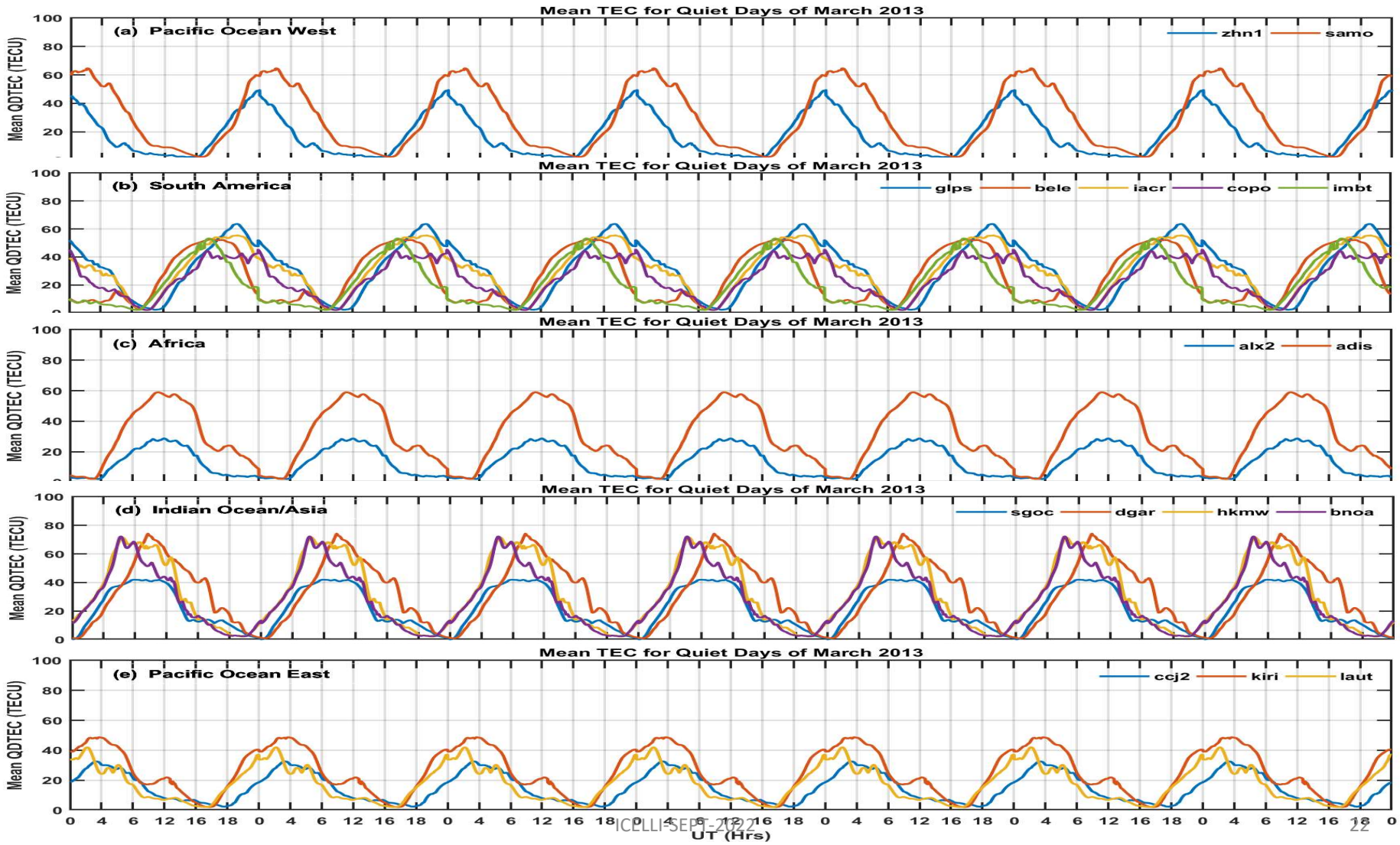
Mean TEC for Quiet Days of March 2013
(a) Pacific Ocean West
zhn1
samo
Mean TEC for Quiet Days of March 2013
(b) South America
glps
bele
iacr
copo
imbt
Mean TEC for Quiet Days of March 2013
(c) Africa
alx2
adis
Mean TEC for Quiet Days of March 2013
(d) Indian Ocean/Asia
sgoc
dgar
hkmw
bnoa
Mean TEC for Quiet Days of March 2013
(e) Pacific Ocean East
ccj2
kiri
laut
Mean QDTEC (TECU)
UT (Hrs)

Storm 1: CME

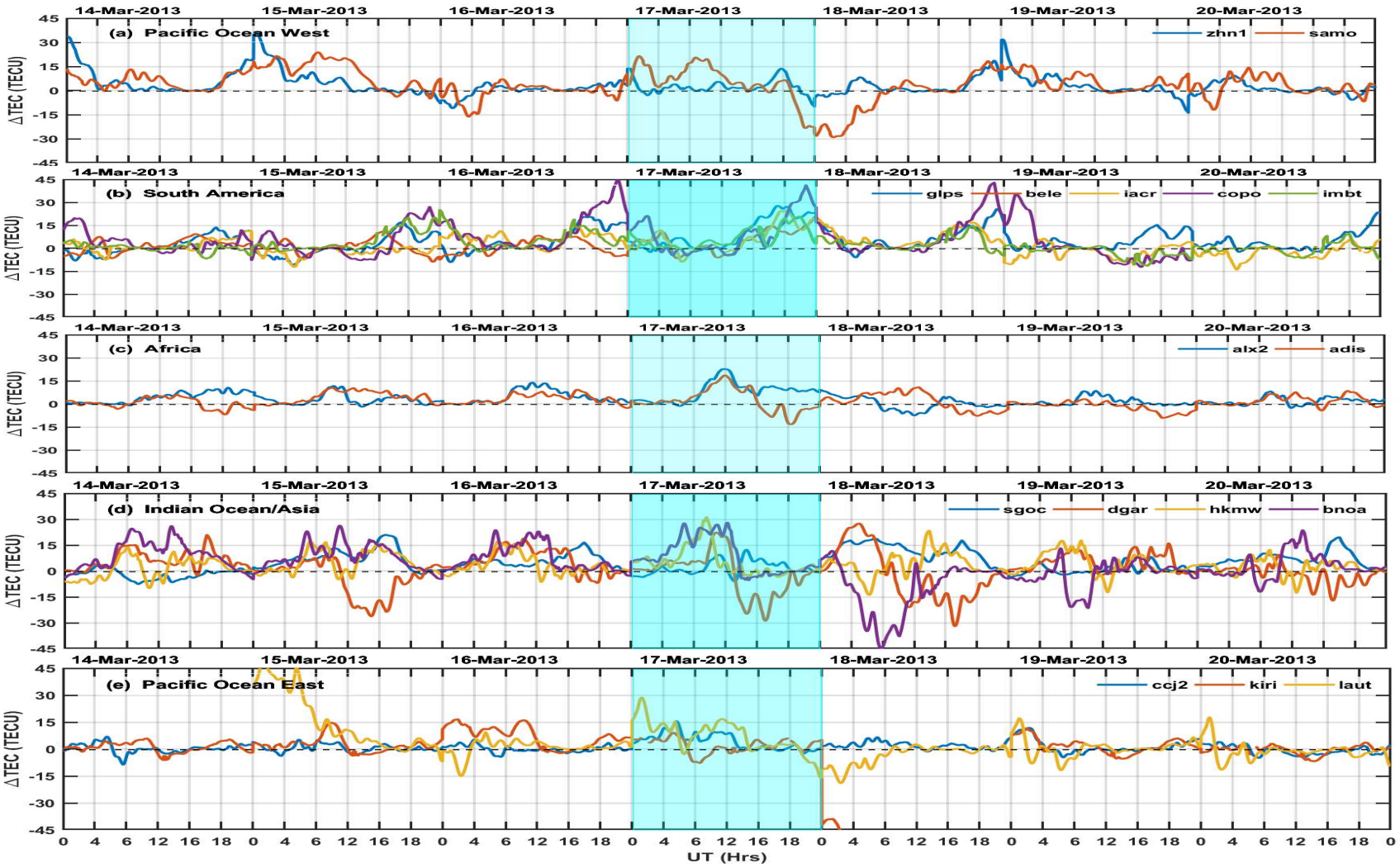
14-Mar-2013
15-Mar-2013
16-Mar-2013
17-Mar-2013
18-Mar-2013
19-Mar-2013
20-Mar-2013
(a) Pacific Ocean West
zhn1
samo
(b) South America
glps
bele
iacr
copo
imbt
(c) Africa
alx2
adis
(d) Indian Ocean/Asia
sgoc
dgar
hkmw
bnoa
(e) Pacific Ocean East
ccj2
kiri
laut
ΔTEC (TECU)
UT (Hrs)

Storm 2: 17 March 2015

CME-driven geomagnetic storm

Storm 2: CME

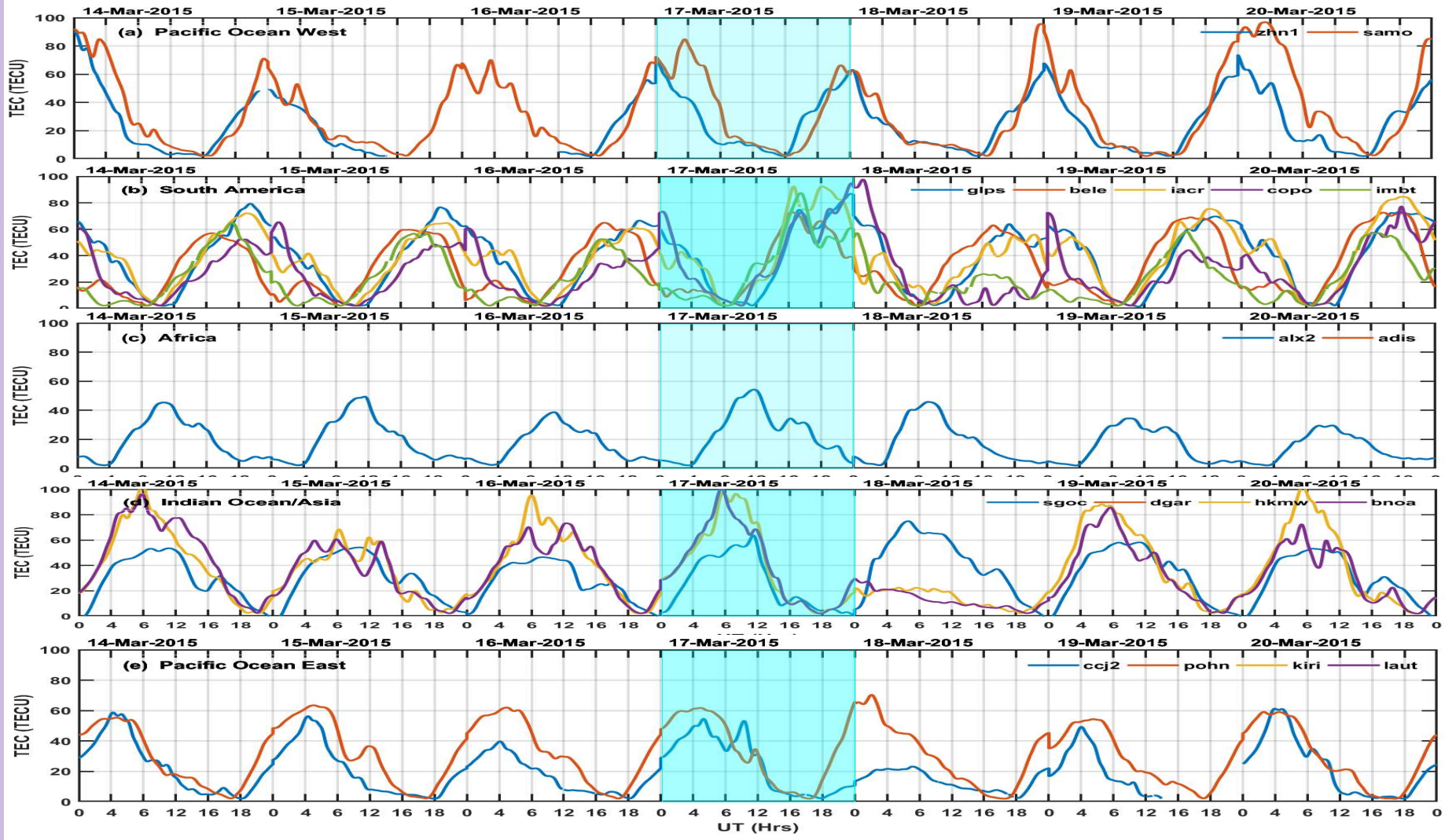

ICELLI-SEPT-2022

Storm 2: CME

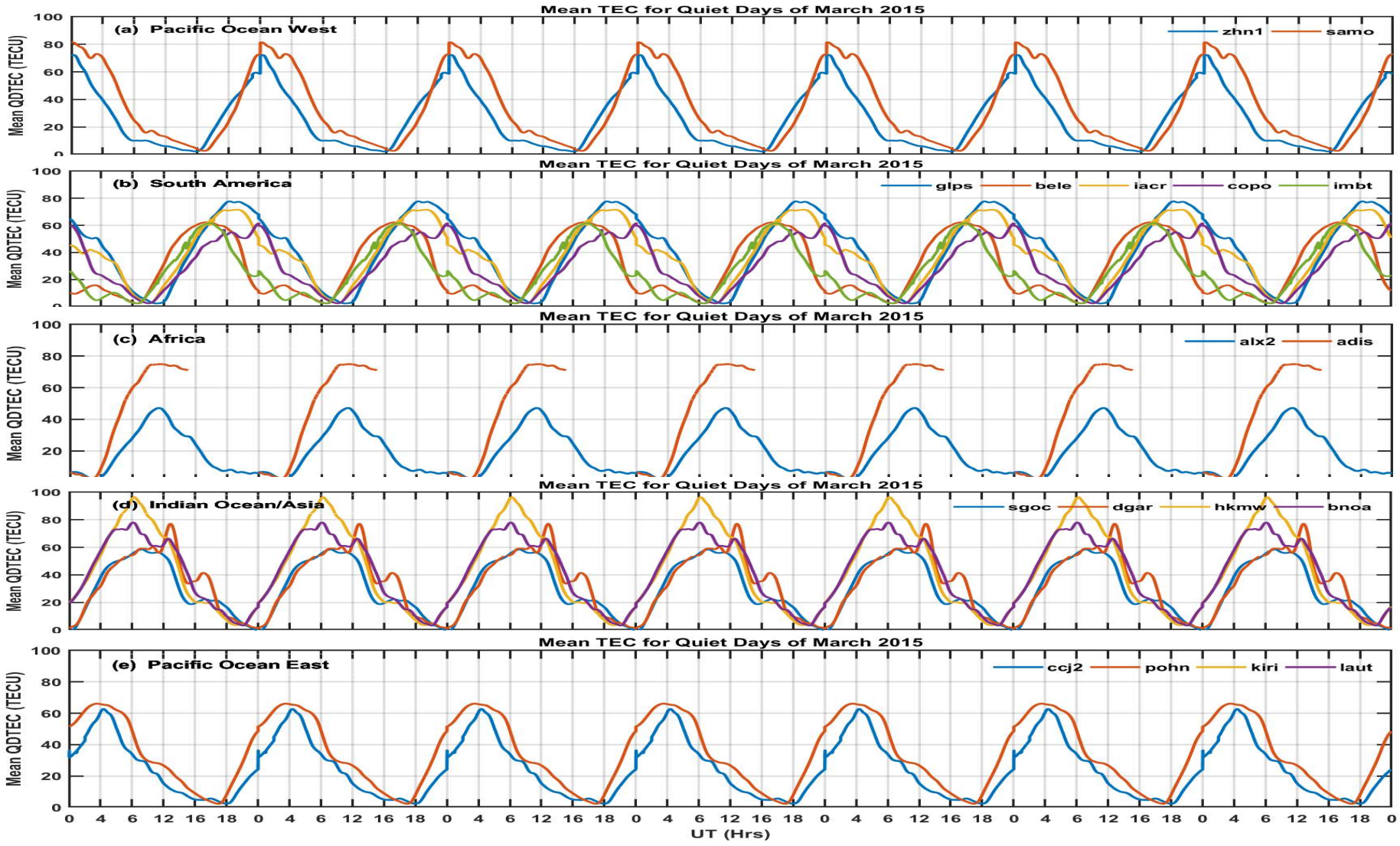

ICELLI-SEPT-2022

Storm 2: CME

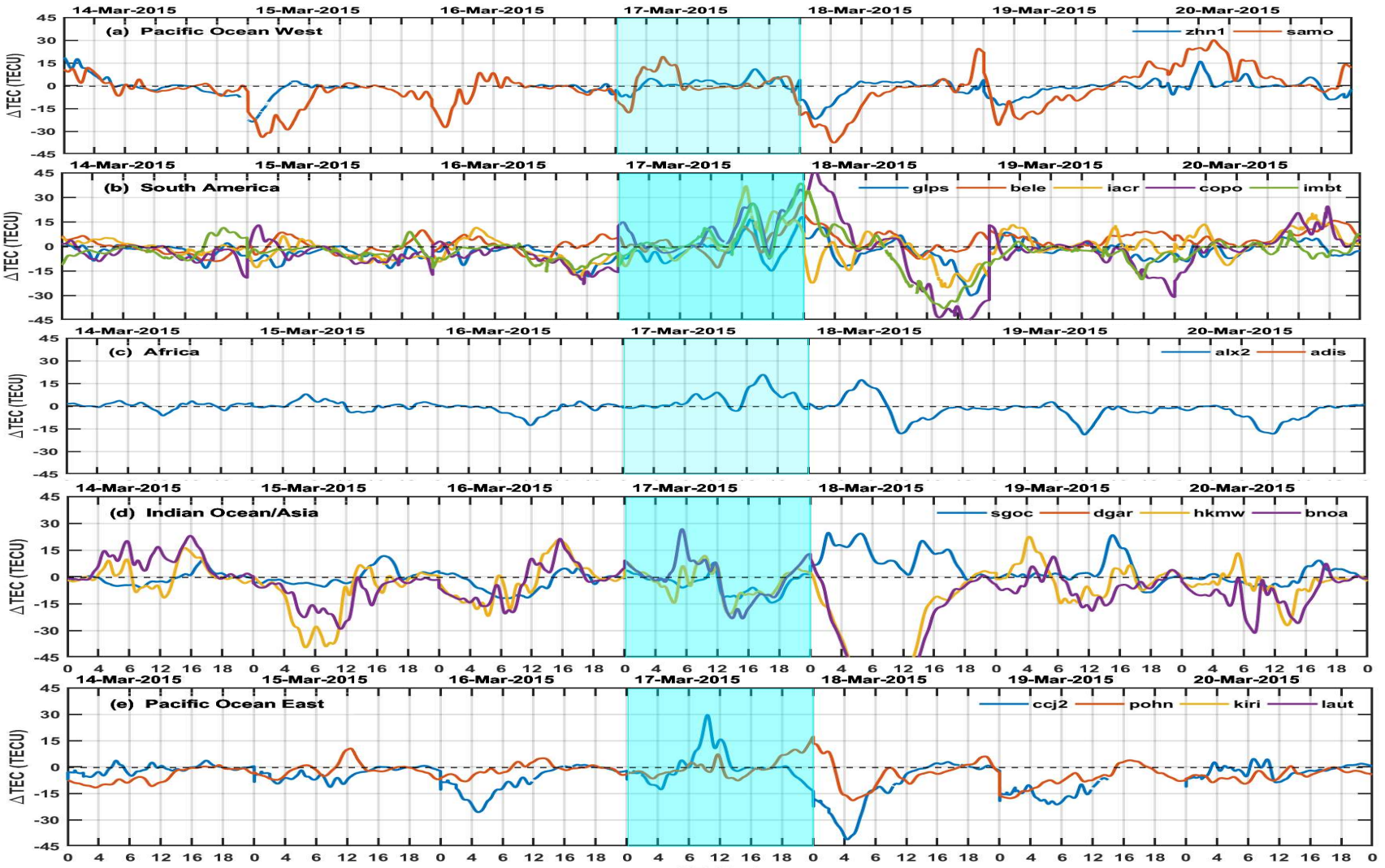
14-Mar-2015
15-Mar-2015
16-Mar-2015
17-Mar-2015
18-Mar-2015
19-Mar-2015
20-Mar-2015
(a) Pacific Ocean West
zhn1
samo
(b) South America
glps
bele
iacr
copo
imbt
(c) Africa
alx2
adis
(d) Indian Ocean/Asia
sgoc
dgar
hkmw
bnoa
(e) Pacific Ocean East
ccj2
pohn
kiri
laut
ΔTEC (TECU)
UT (hrs)

Storm 3: 1 June 2013

CIR-driven geomagnetic storm

Storm 3: CIR

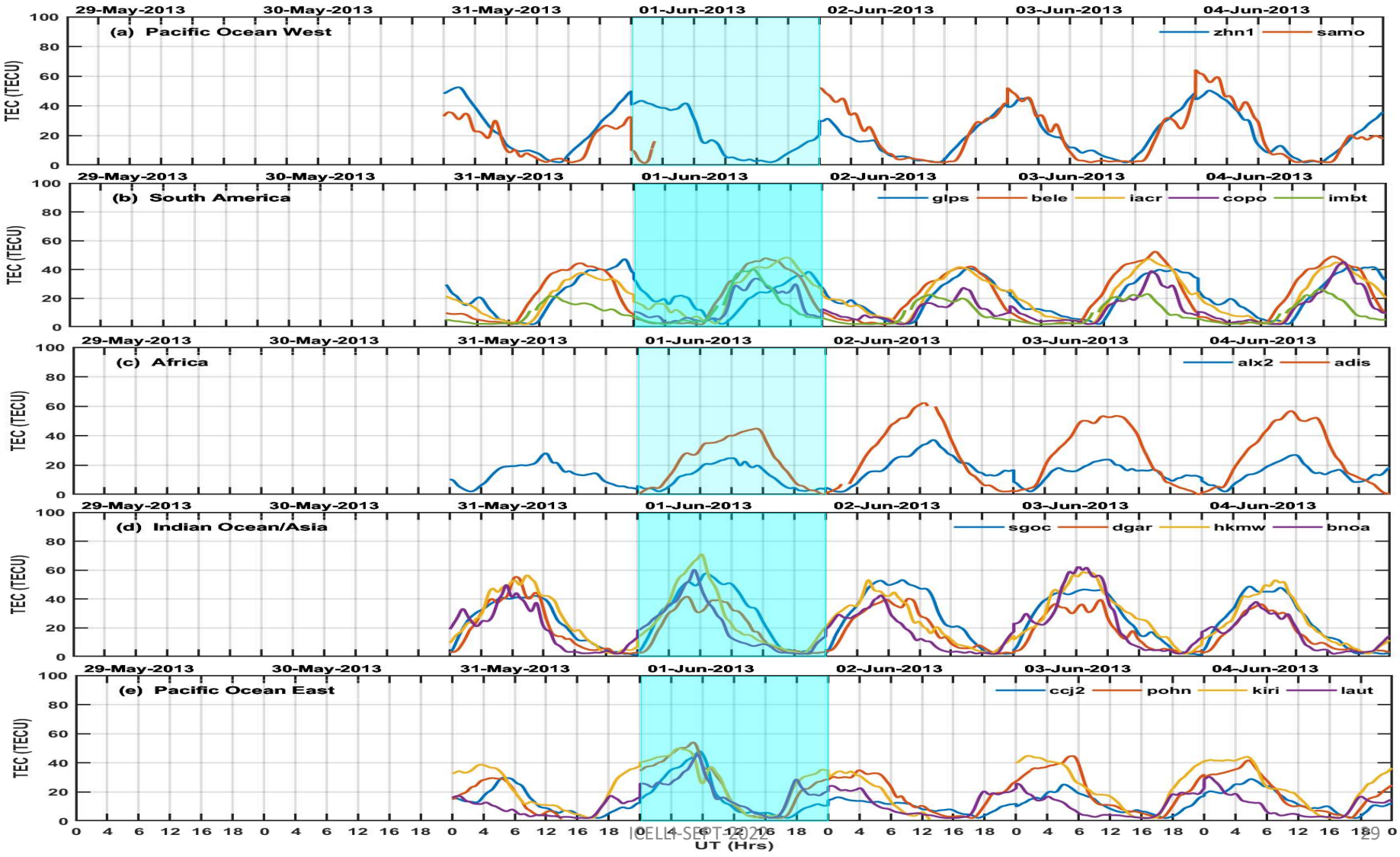
29-May-2013
30-May-2013
31-May-2013
01-Jun-2013
02-Jun-2013
03-Jun-2013
04-Jun-2013
(a) Pacific Ocean West
zhn1
samo
(b) South America
glps
bele
iacr
copo
imbt
(c) Africa
alx2
adis
(d) Indian Ocean/Asia
sgoc
dgar
hkmw
bnoa
(e) Pacific Ocean East
ccj2
pohn
kiri
laut
TEC (TECU)
UT (Hrs)

Storm 3: CIR

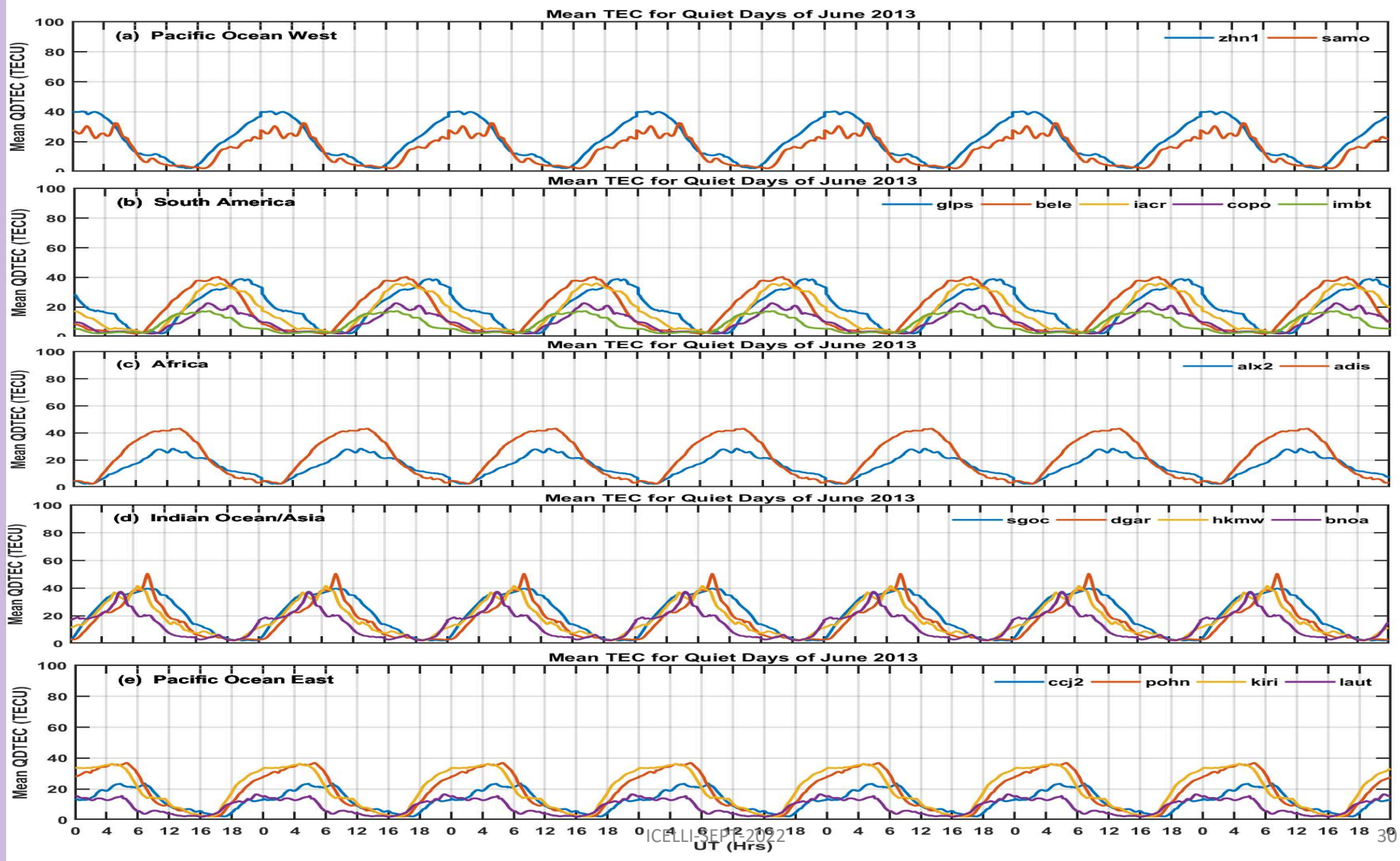
Mean TEC for Quiet Days of June 2013
(a) Pacific Ocean West
zhn1
samo
Mean TEC for Quiet Days of June 2013
(b) South America
glps
bele
iacr
copo
imbt
Mean TEC for Quiet Days of June 2013
(c) Africa
alx2
adis
Mean TEC for Quiet Days of June 2013
(d) Indian Ocean/Asia
sgoc
dgar
hkmw
bnoa
Mean TEC for Quiet Days of June 2013
(e) Pacific Ocean East
ccj2
pohn
kiri
laut
Mean QDTEC (TECU)
UT (Hrs)

Storm 3: CIR

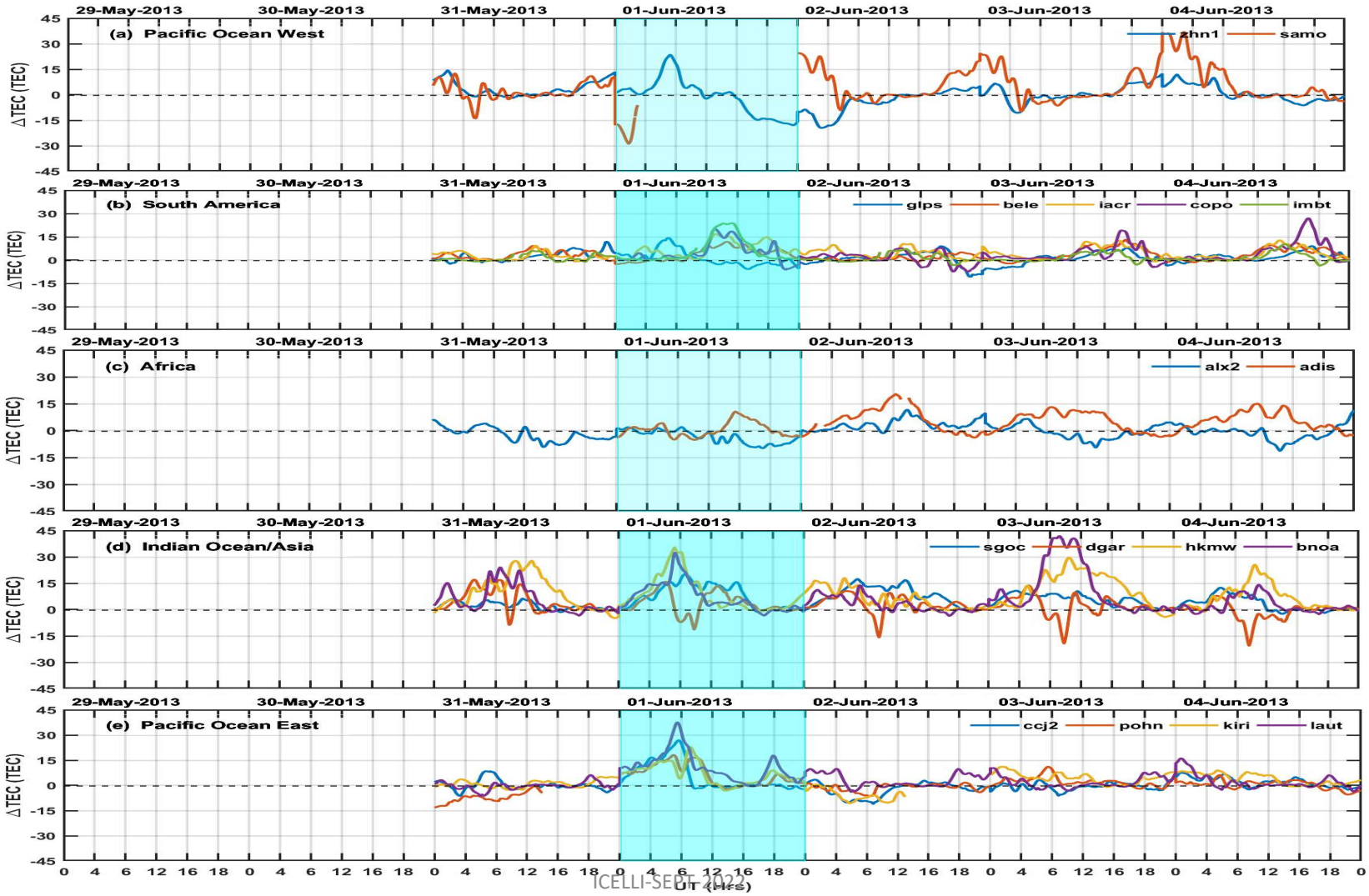
29-May-2013
30-May-2013
31-May-2013
01-Jun-2013
02-Jun-2013
03-Jun-2013
04-Jun-2013
(a) Pacific Ocean West
zhn1
samo
(b) South America
glps
bele
iacr
copo
imbt
(c) Africa
alx2
adis
(d) Indian Ocean/Asia
sgoc
dgar
hkmw
bnoa
(e) Pacific Ocean East
ccj2
pohn
kiri
laut
ΔTEC (TEC)
UT (Hrs)

Storm 4: 7 October 2015

CIR-driven geomagnetic storm

Storm 4: CIR

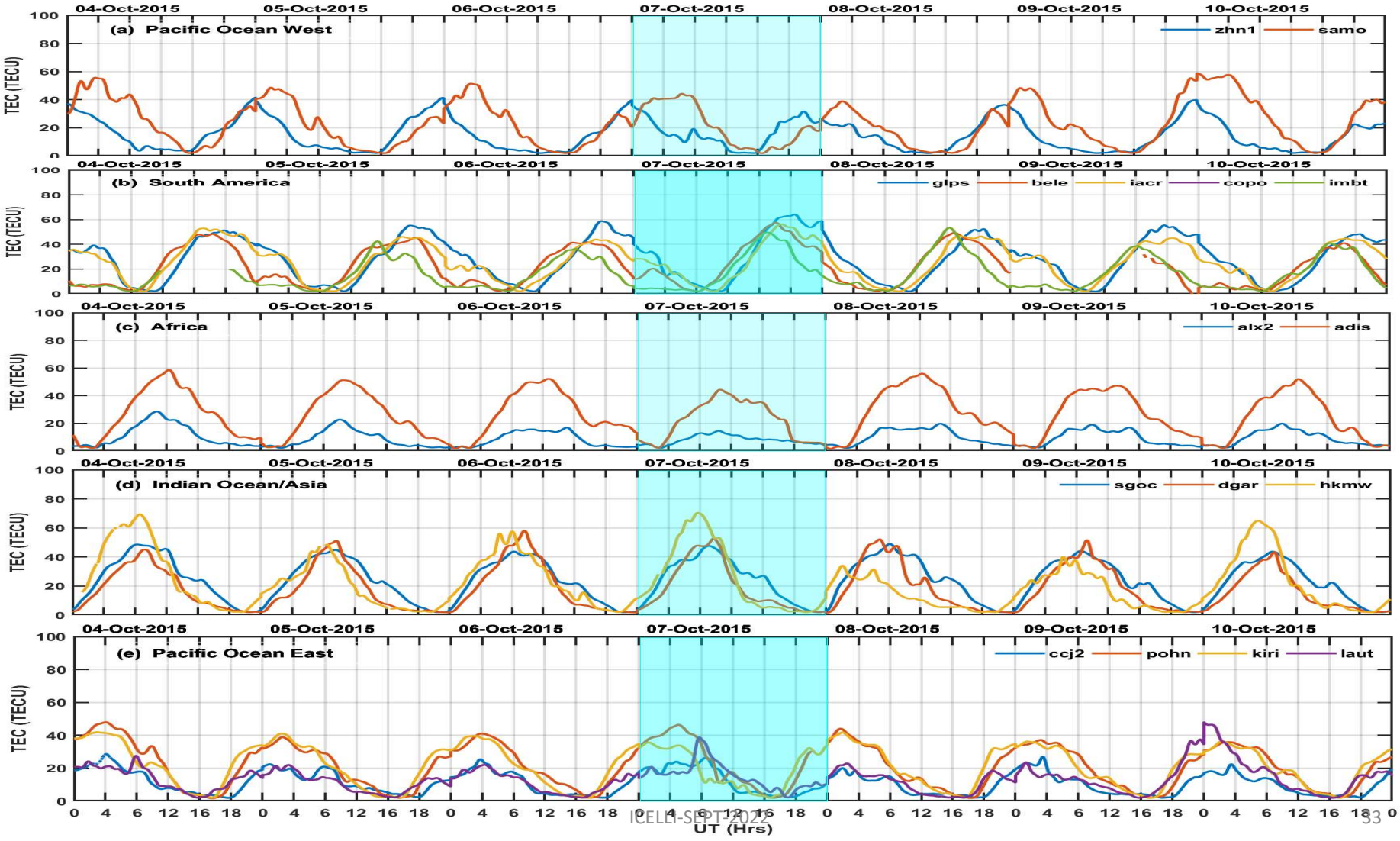
04-Oct-2015
05-Oct-2015
06-Oct-2015
07-Oct-2015
08-Oct-2015
09-Oct-2015
10-Oct-2015
(a) Pacific Ocean West
zhn1
samo
(b) South America
glps
bele
iacr
copo
imbt
(c) Africa
alx2
adis
(d) Indian Ocean/Asia
sgoc
dgar
hkmw
(e) Pacific Ocean East
ccj2
pohn
kiri
laut
TEC (TECU)
UT (Hrs)

Storm 4: CIR

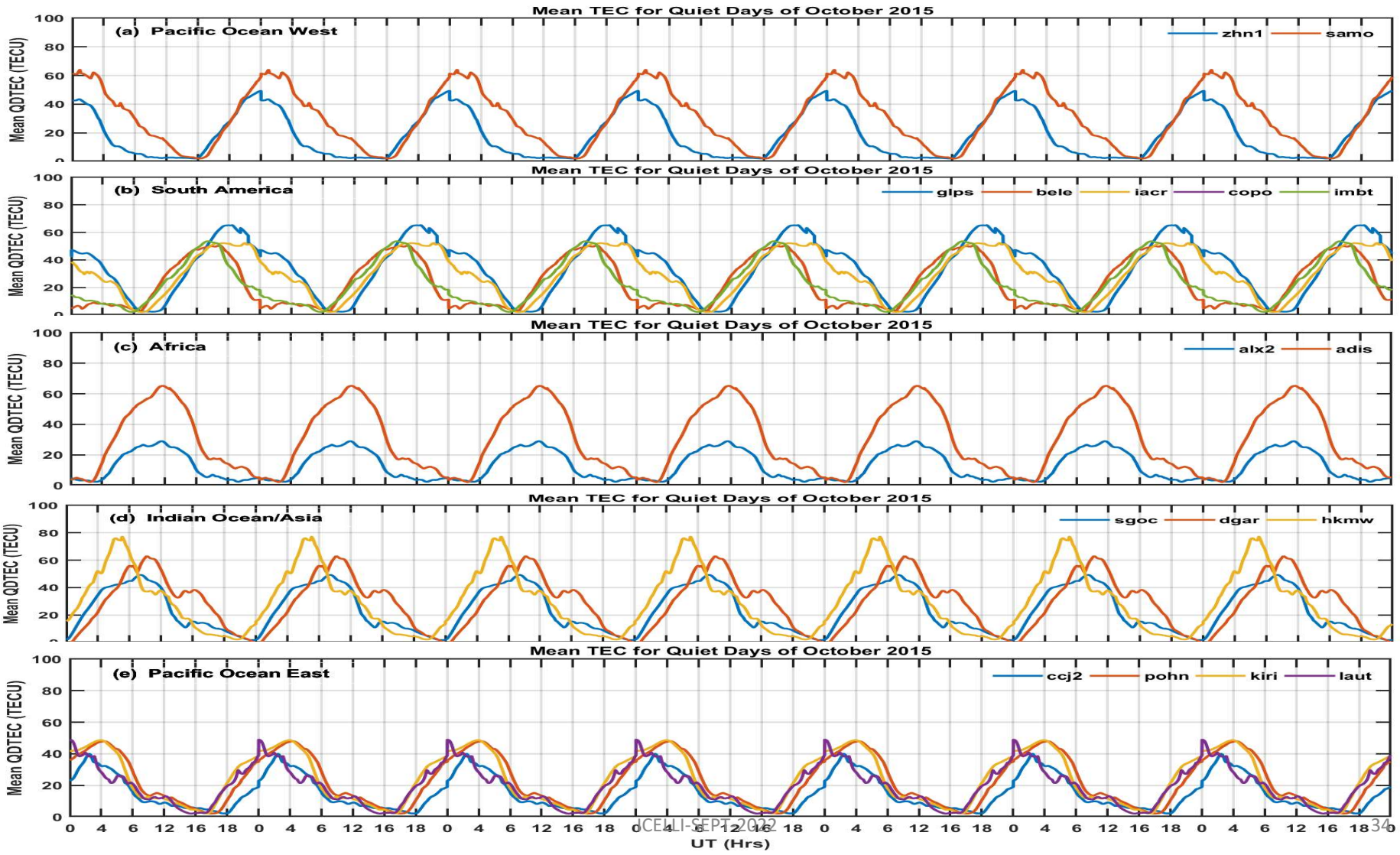
Mean TEC for Quiet Days of October 2015
(a) Pacific Ocean West
zhn1
samo
Mean TEC for Quiet Days of October 2015
(b) South America
glps
bele
iacr
copo
imbt
Mean TEC for Quiet Days of October 2015
(c) Africa
alx2
adis
Mean TEC for Quiet Days of October 2015
(d) Indian Ocean/Asia
sgoc
dgar
hkmw
Mean TEC for Quiet Days of October 2015
(e) Pacific Ocean East
ccj2
pohn
kiri
laut
Mean QDTEC (TECU)
UT (Hrs)

Storm 4: CIR

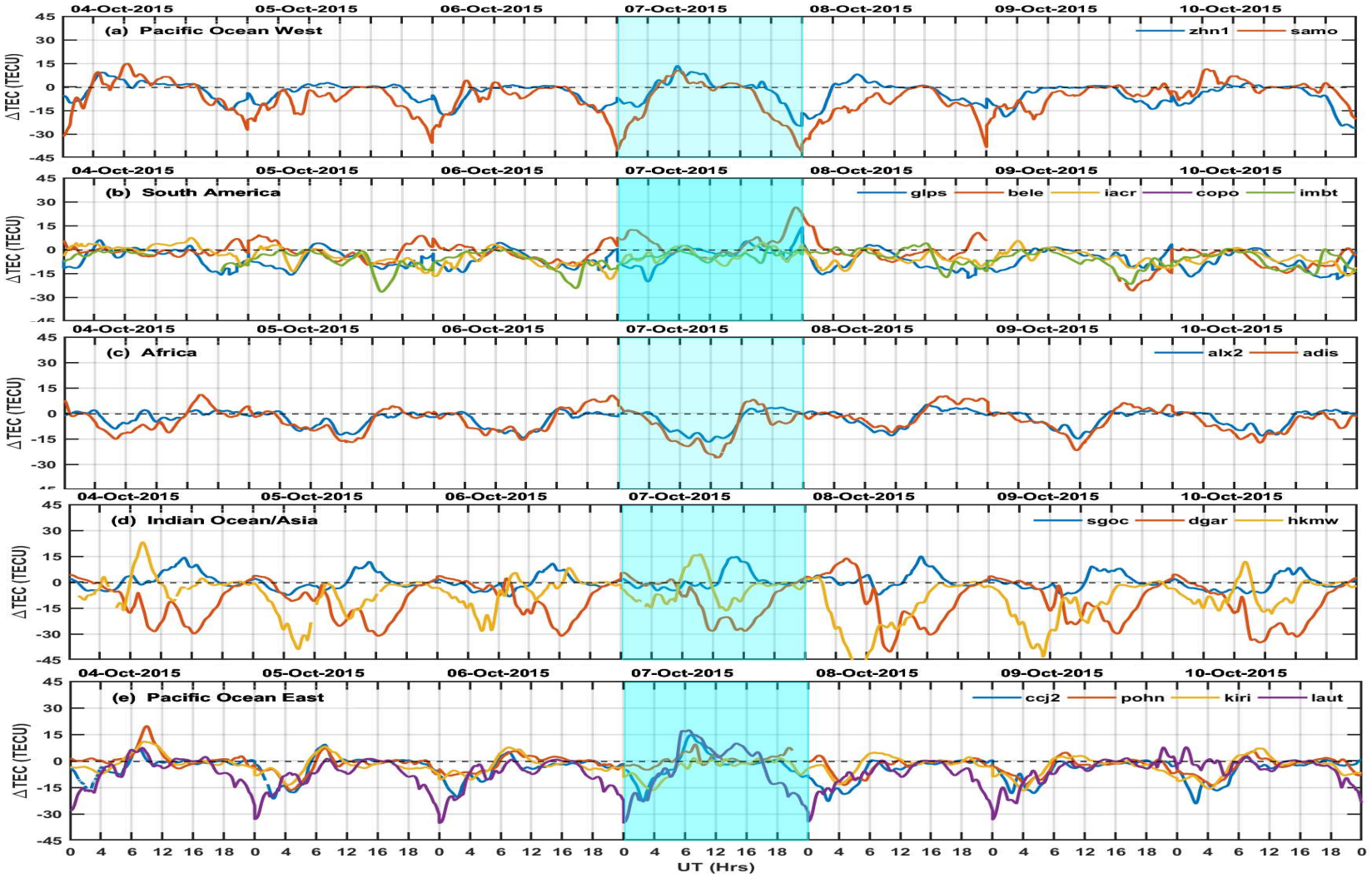
04-Oct-2015
05-Oct-2015
06-Oct-2015
07-Oct-2015
08-Oct-2015
09-Oct-2015
10-Oct-2015
(a) Pacific Ocean West
zhn1
samo
(b) South America
glps
bele
iacr
copo
imbt
(c) Africa
alx2
adis
(d) Indian Ocean/Asia
sgoc
dgar
hkmw
(e) Pacific Ocean East
ccj2
pohn
kiri
laut
ΔTEC (TECU)
UT (Hrs)

ROTI as Proxy for Ionospheric Irregularities for the 17 March 2013 CME Storm

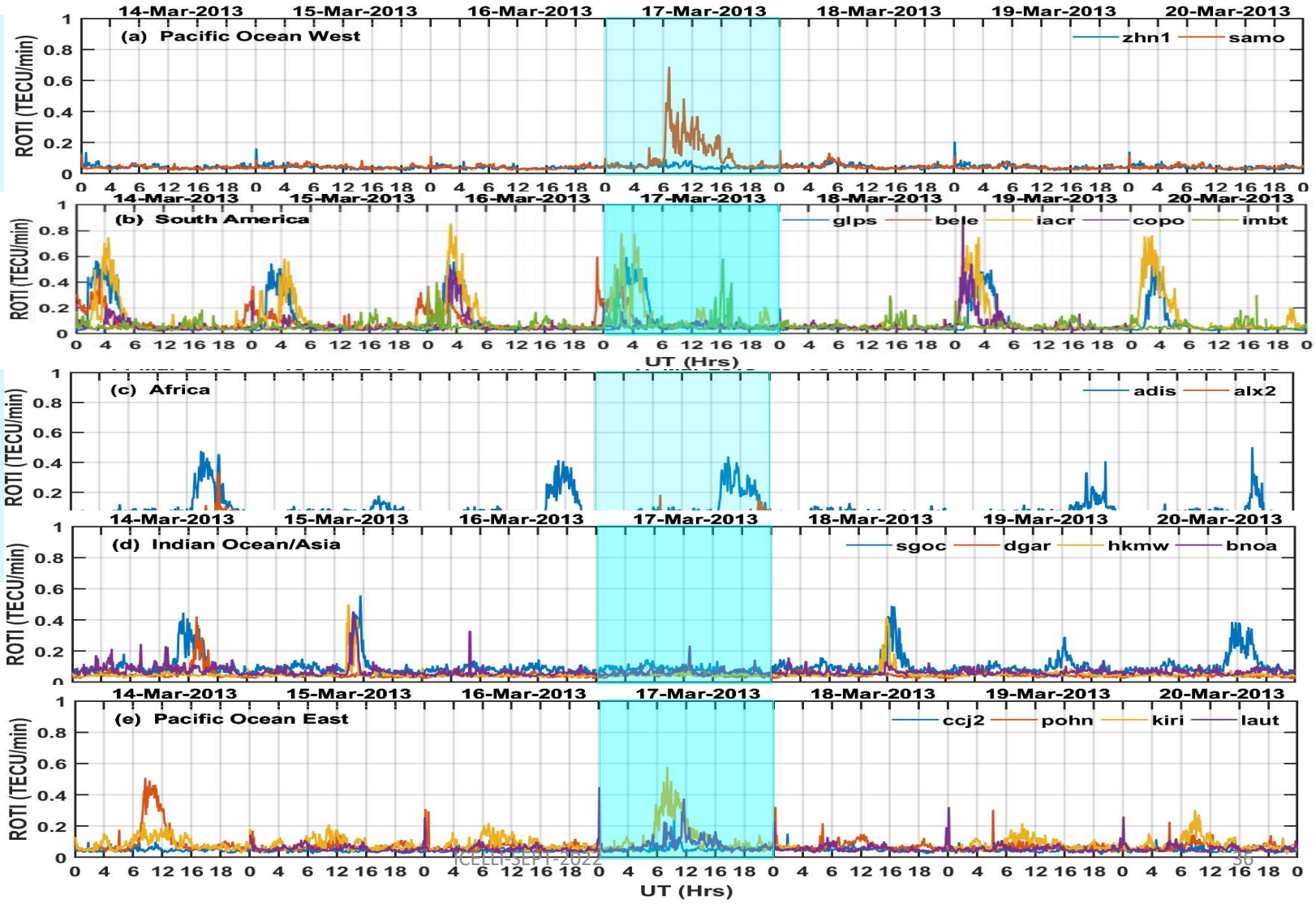

ROTI as Proxy for Ionospheric Irregularities for the 17 March 2015 CME Storm

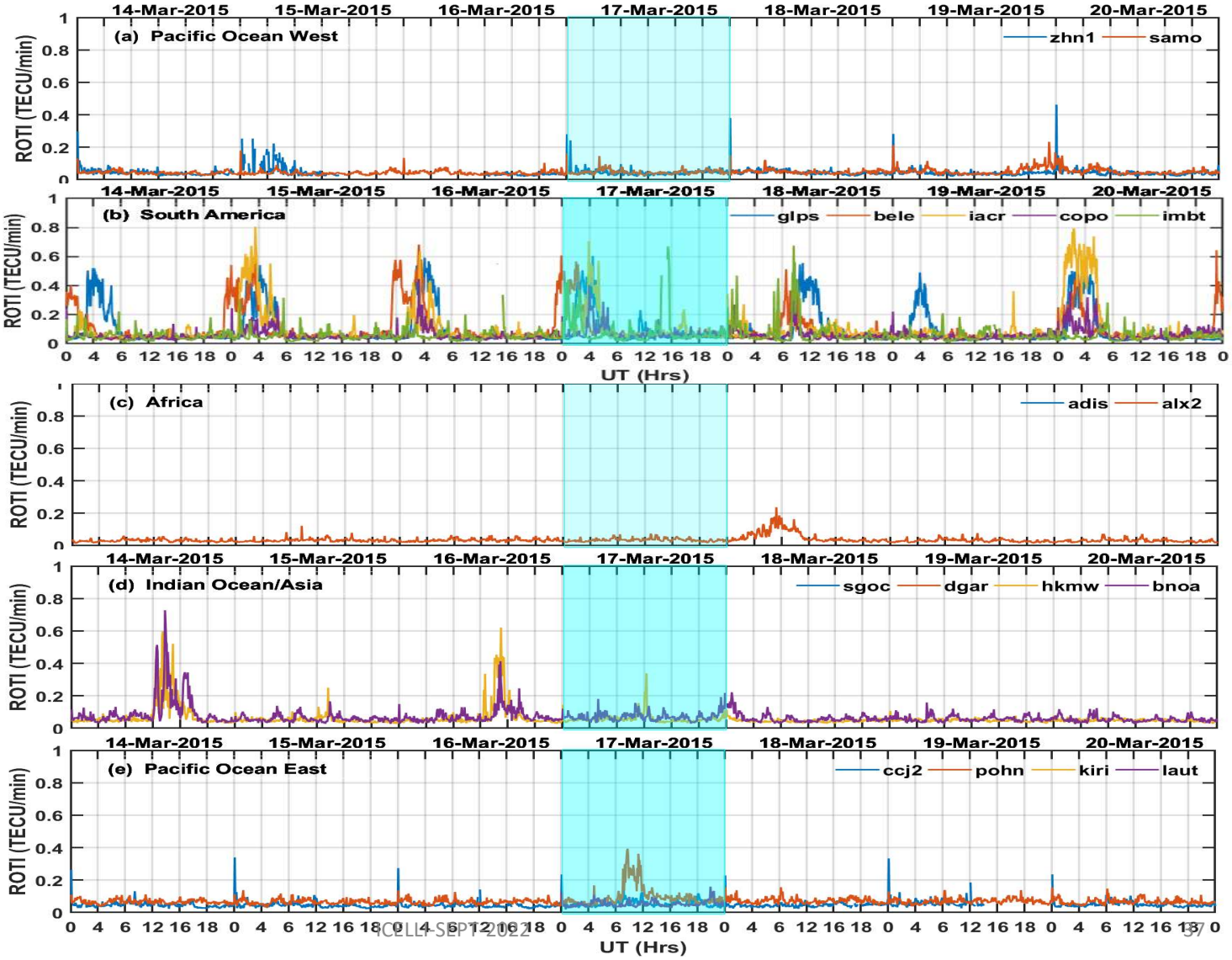

Validation of ROTI Results with ISEE Global ROTI Maps

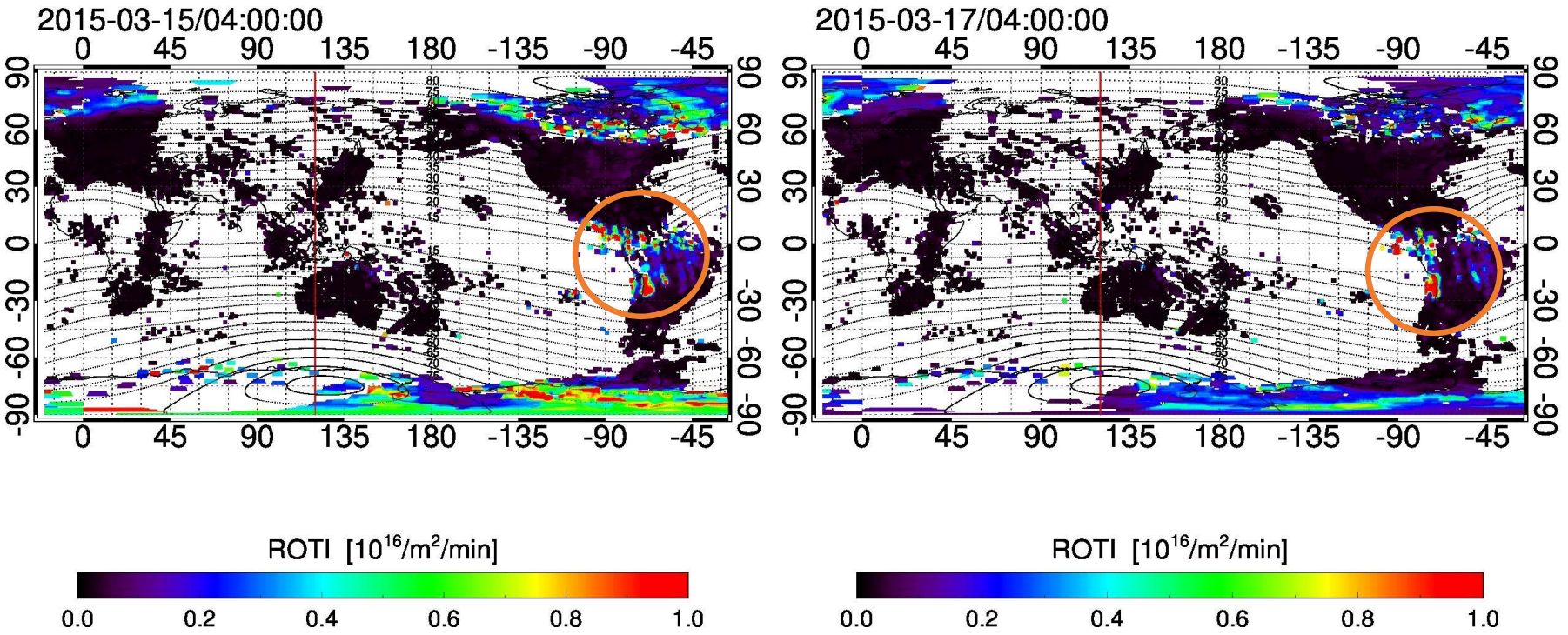

ICELLI-SEPT-2022

ROTI as Proxy for Ionospheric Irregularities for the 1 June 2013 CIR Storm

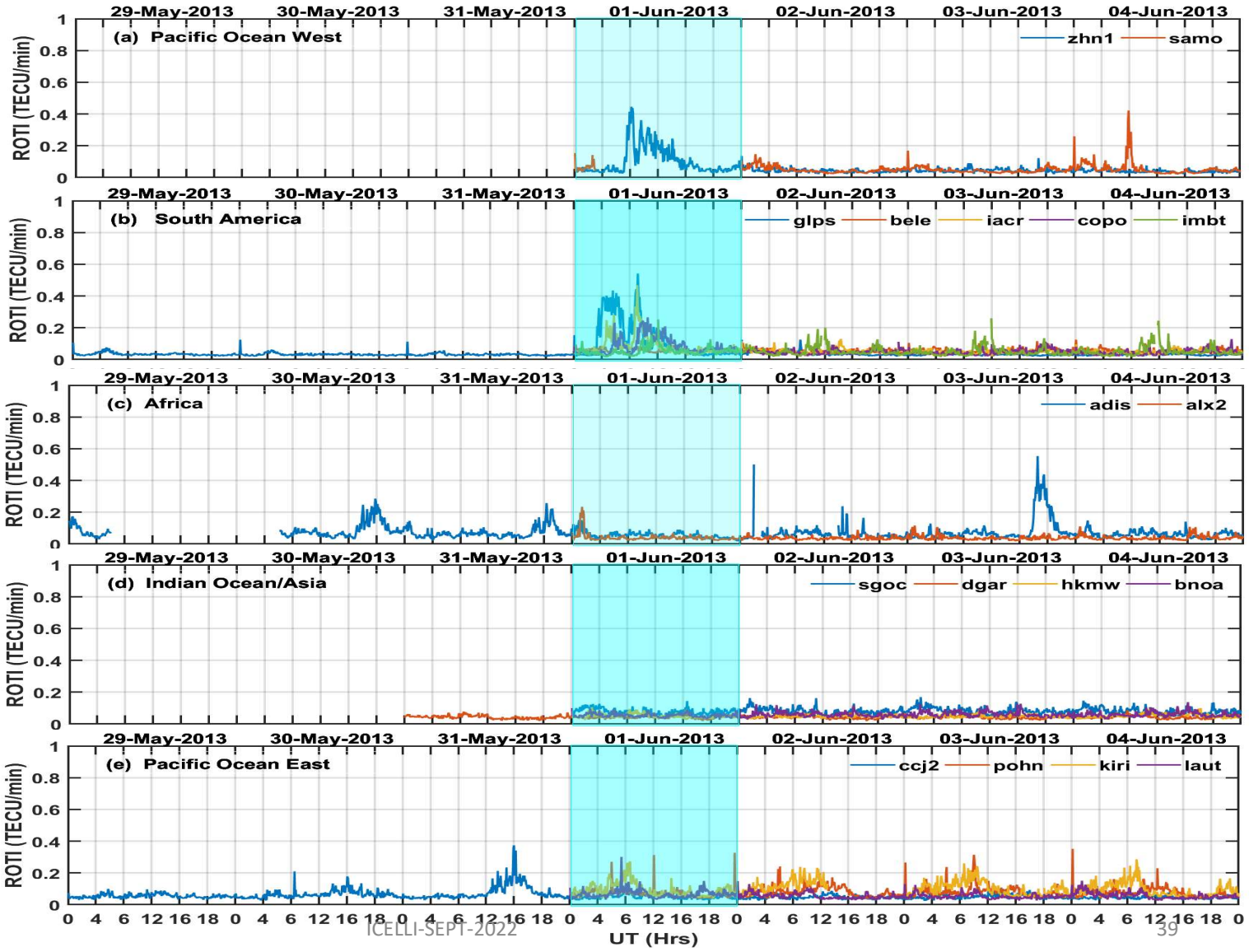

ROTI as Proxy for Ionospheric Irregularities for the 7 October 2015 CIR Storm

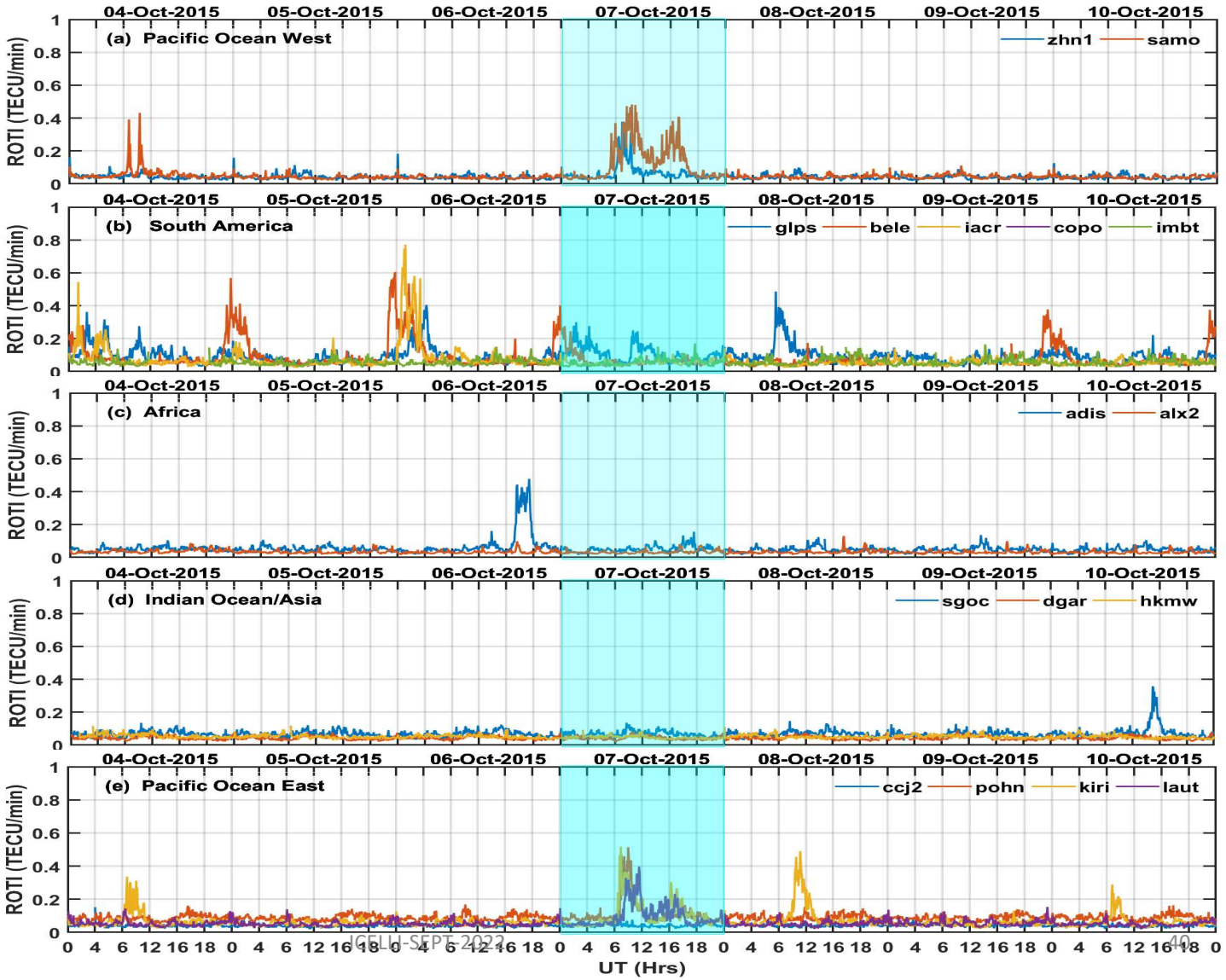

Table 2: Properties of the geomagnetic storms

S/N	Date of Initial, Main, Recovery Phases	Min Dst (nT)	IP Driver	Onset (Min Dst) UT	Pacific Ocean West LT =~-10+UT	South America LT =~-3+UT	Africa LT =~3+UT	Indian Ocean/Asia LT =~7+UT	Pacific Ocean East LT =~11+UT
1.	17/03/13	-134	CME	0600(2000)	2000(1000)	0300(1700)	0900(2300)	1300(0300)	1700(0700)
2.	01/06/13	-124	CIR	0600(2000)	2000(1000)	0300(1700)	0900(2300)	1300(0300)	1700(0700)
3.	17/03/15	-222	CME	0600(2100)	2000(1100)	0300(1800)	0900(0000)	1300(0400)	1700(0800)
4.	07/10/15	-124	CIR	0200(2100)	1600(1100)	2300(1800)	0500(0000)	0900(0400)	1400(0800)

Low-latitude ionosphere: At sunset, Pre Reversal Enhancement (PRE) lifts up the ionosphere to a conducive altitude where irregularities are generated through R-T instability mechanism (Kelley, 1989). To this end, geomagnetic storm with onset time or time of minimum Dst at sunset/post-sunset hours generates more irregularities.

E X B Drift

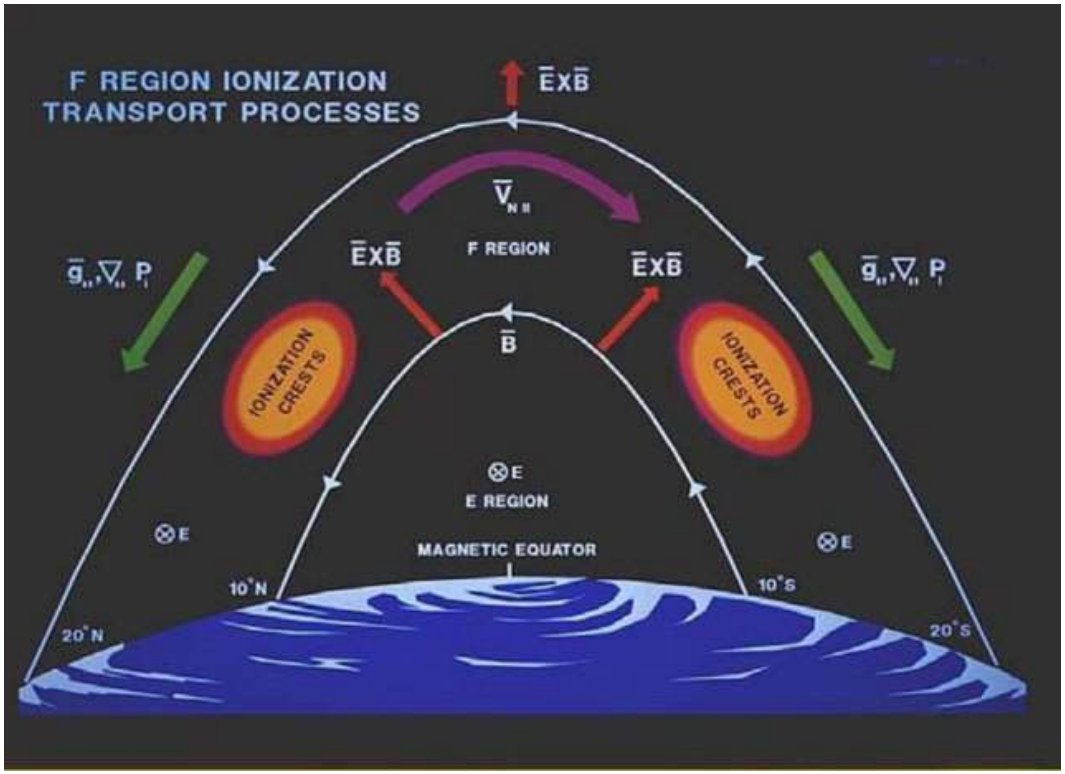
F REGION IONIZATION
TRANSPORT PROCESSES
ĒXB̄
V̄N ⊥
ĒXB̄
F REGION
ĒXB̄
ḡ⊥,∇⊥ Pi
ḡ⊥,∇⊥ Pi
IONIZATION CRESTS
IONIZATION CRESTS
B̄
⊗E
E REGION
⊗E
⊗E
MAGNETIC EQUATOR
10°N
10°S
20°N
20°S

O/N2 Thermospheric Ratio for 17 March 2013 CME Storm

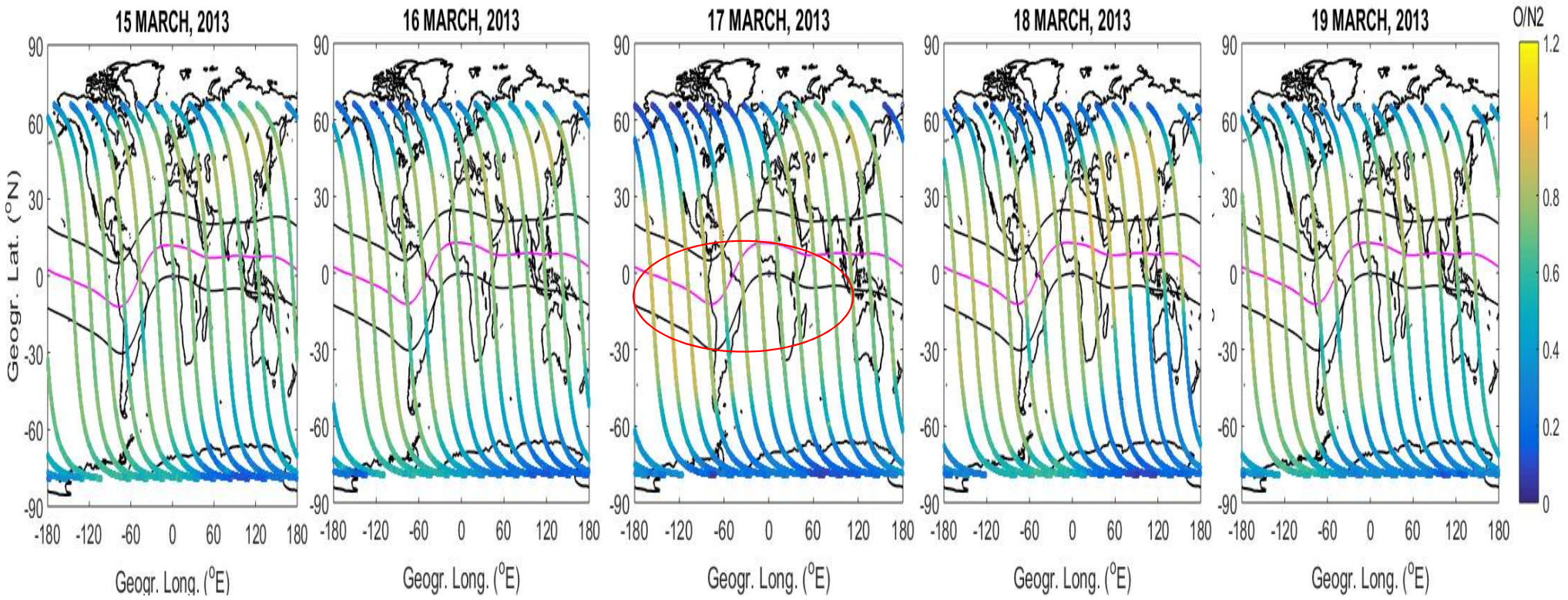

O/N2 Thermospheric Ratio for 1 June 2013 CME Storm

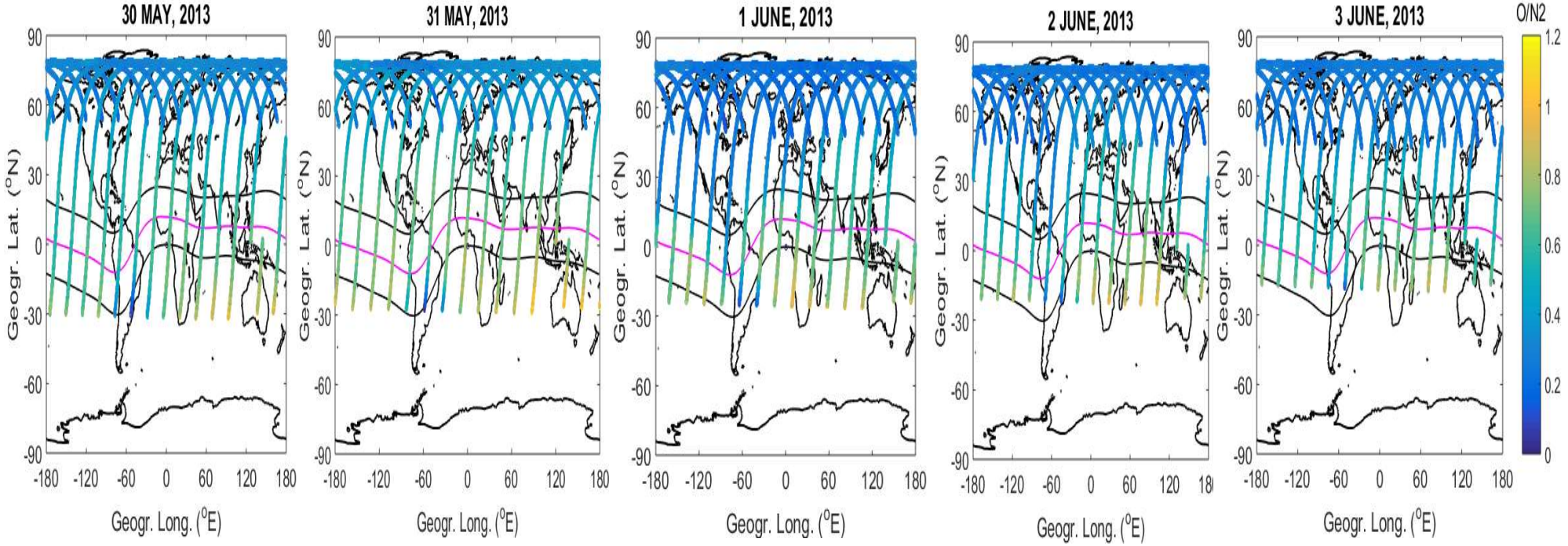

O/N2 Thermospheric Ratio for 17 March 2015 CME Storm

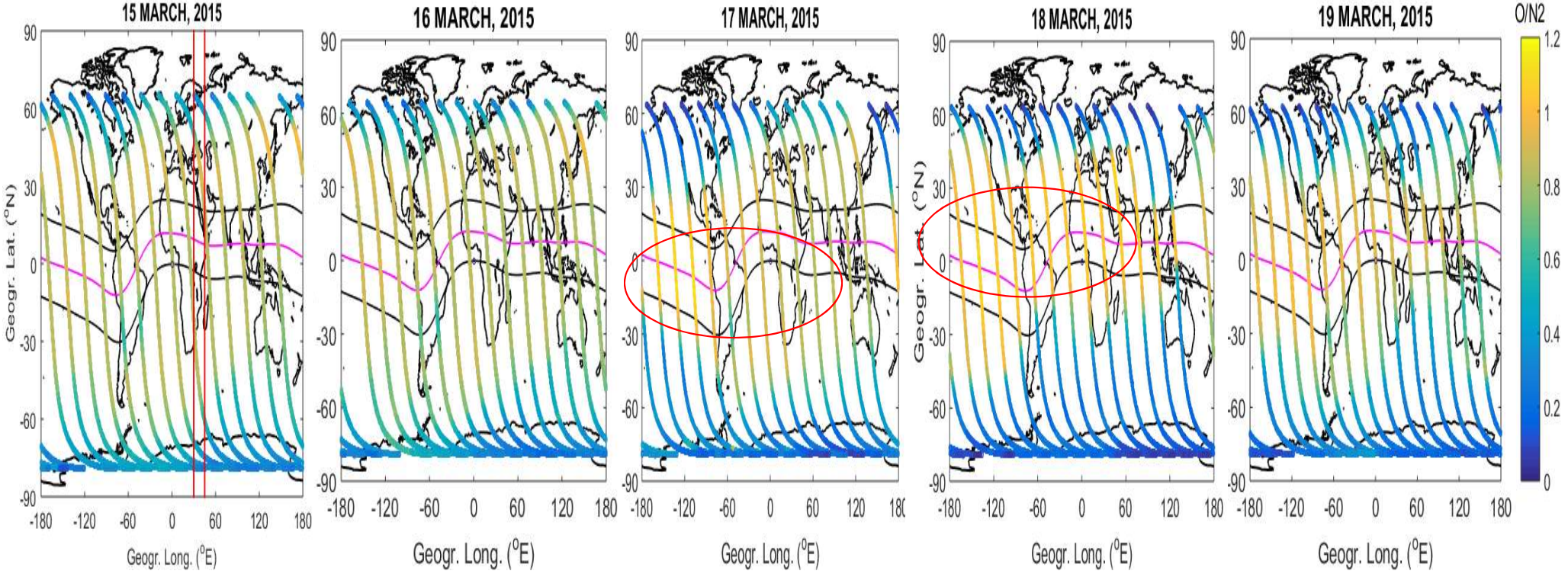

Interpretation of O/N2 results

High O/N_2 ratio implies low recombination processes in the ionosphere, leading to high plasma densities, while low O/N_2 ratio implies enhanced recombination processes in the ionosphere, leading to low plasma densities (Fuller-Rowell et al., 1994).

SuperMag H Data: CIR GS

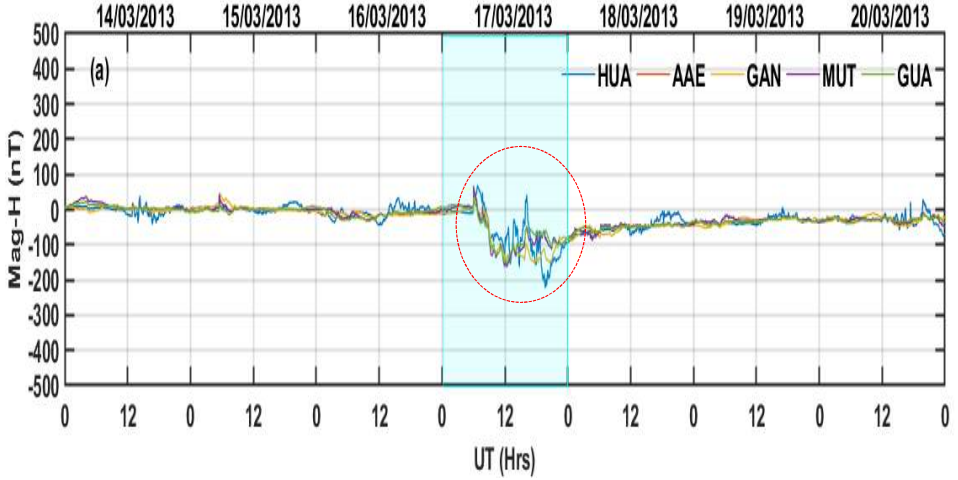

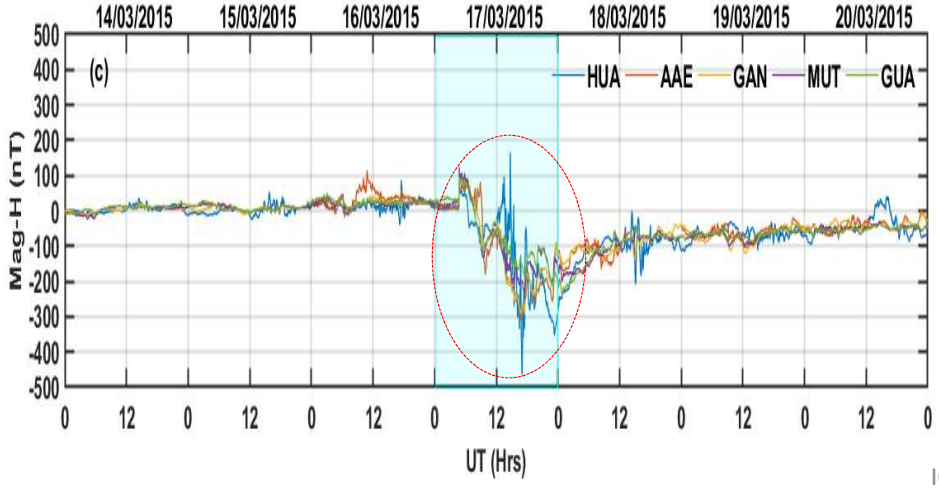

SuperMag H Data: CME GS

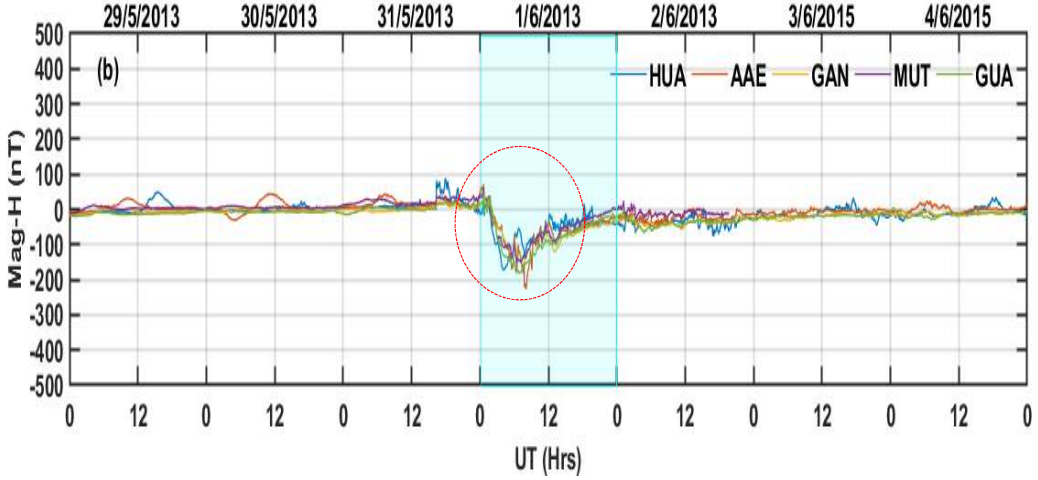

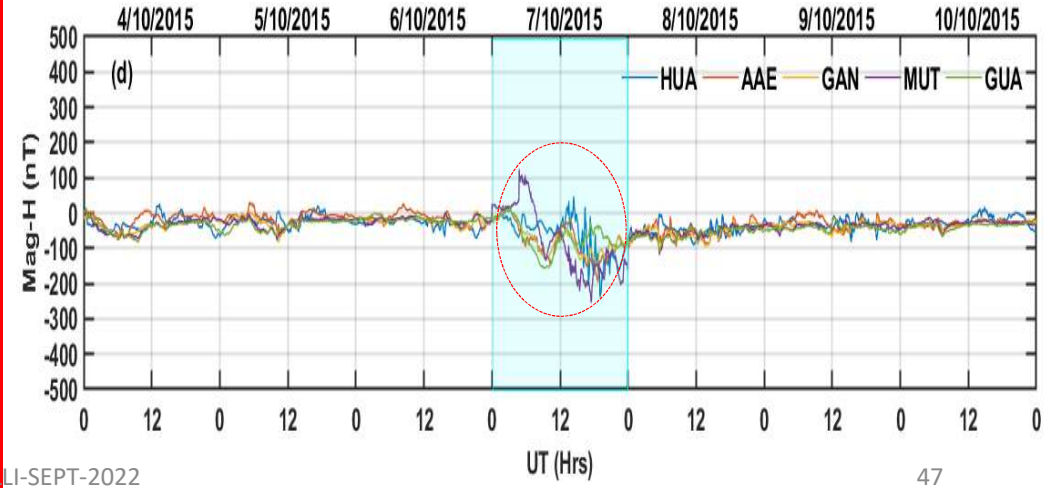

CME G-Storms

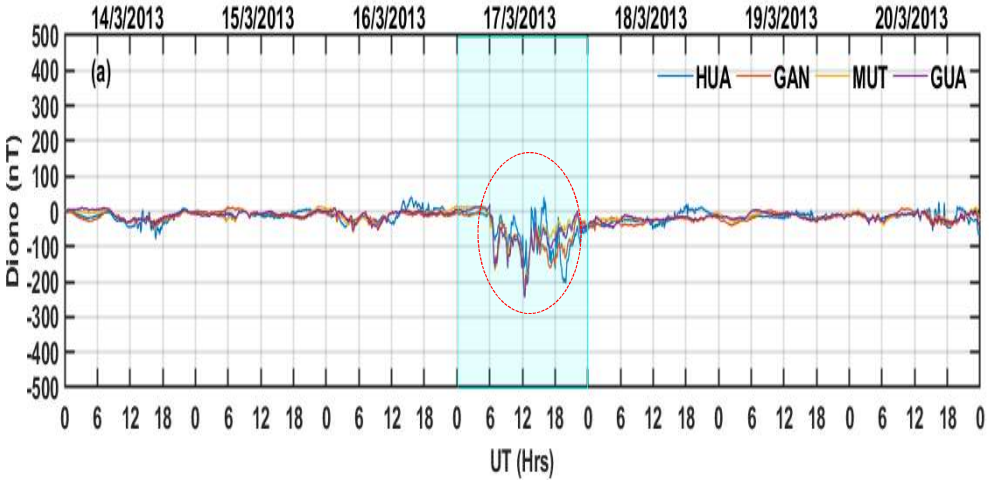

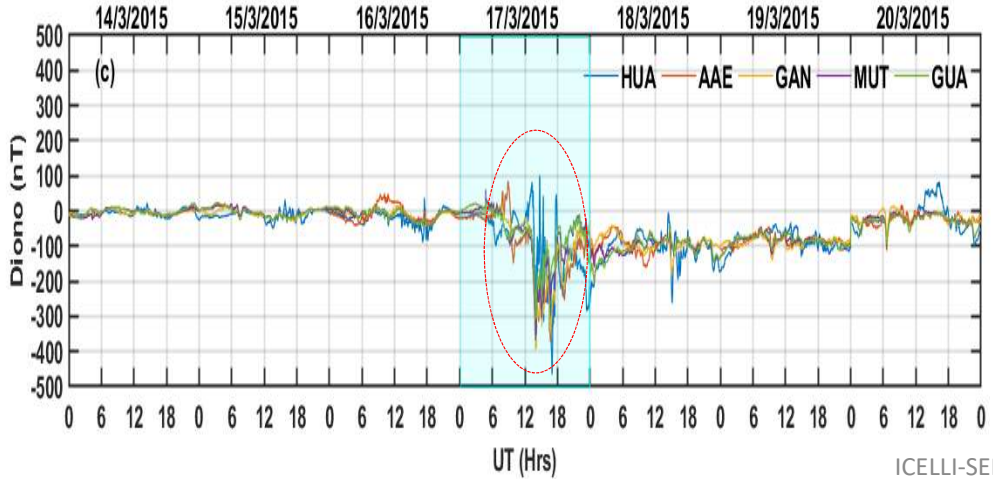

CIR G-Storms

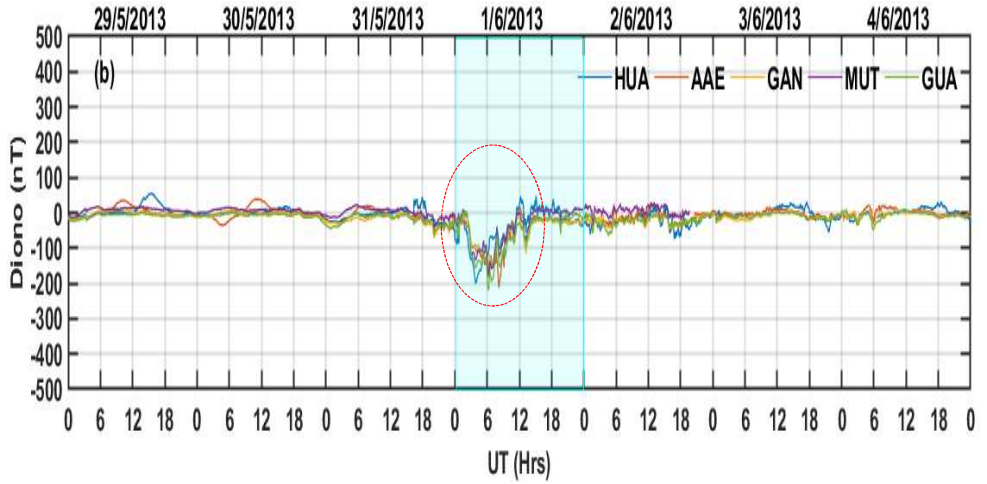

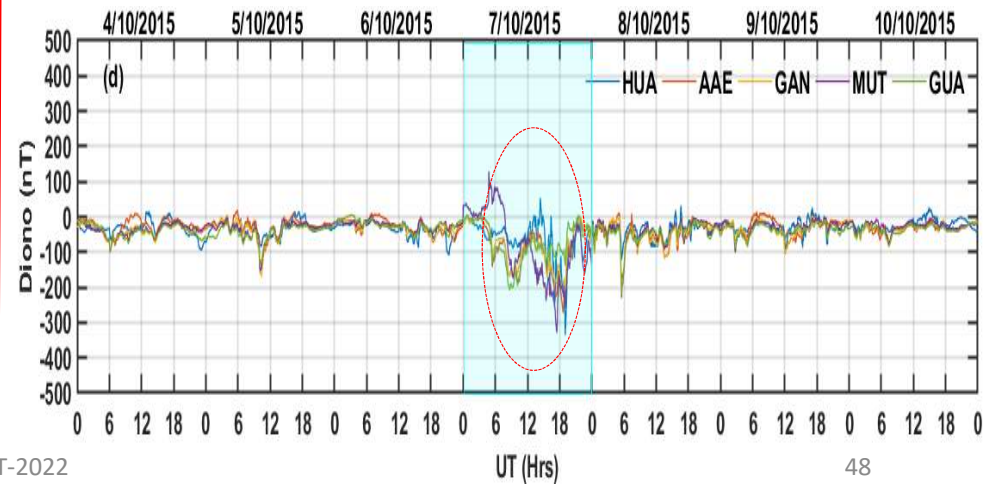

CME G-Storms

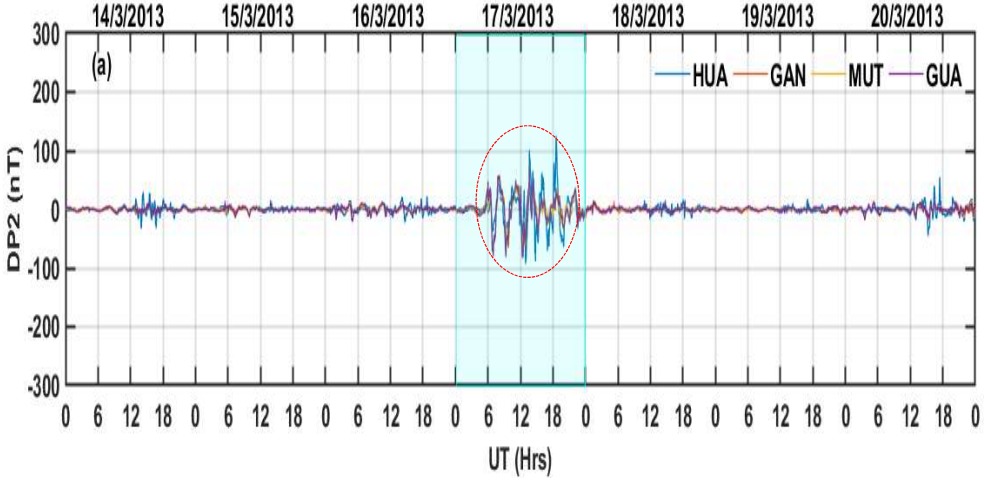

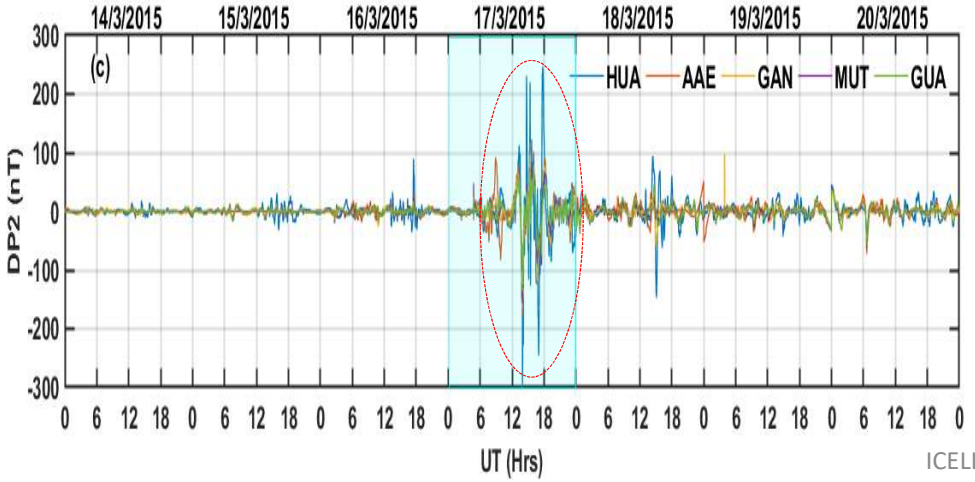

CIR G-Storms

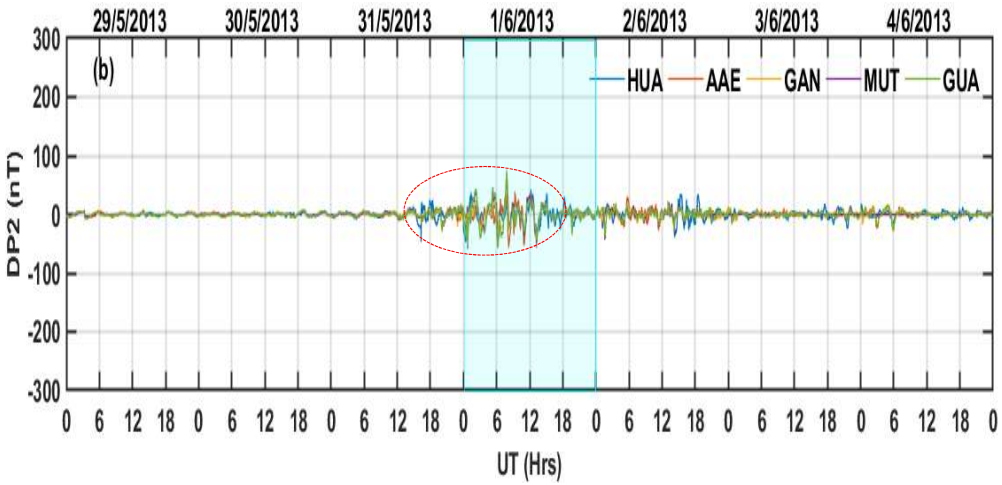

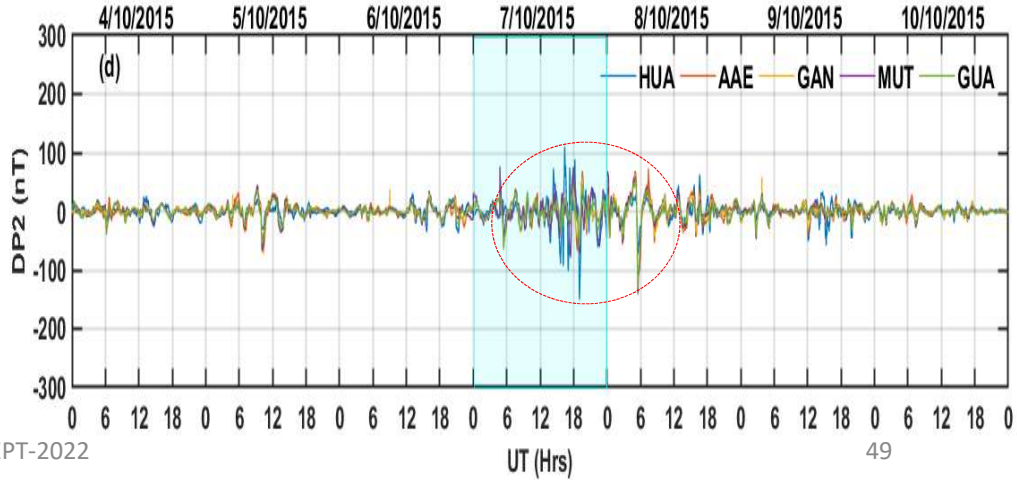

CME G-Storms Model

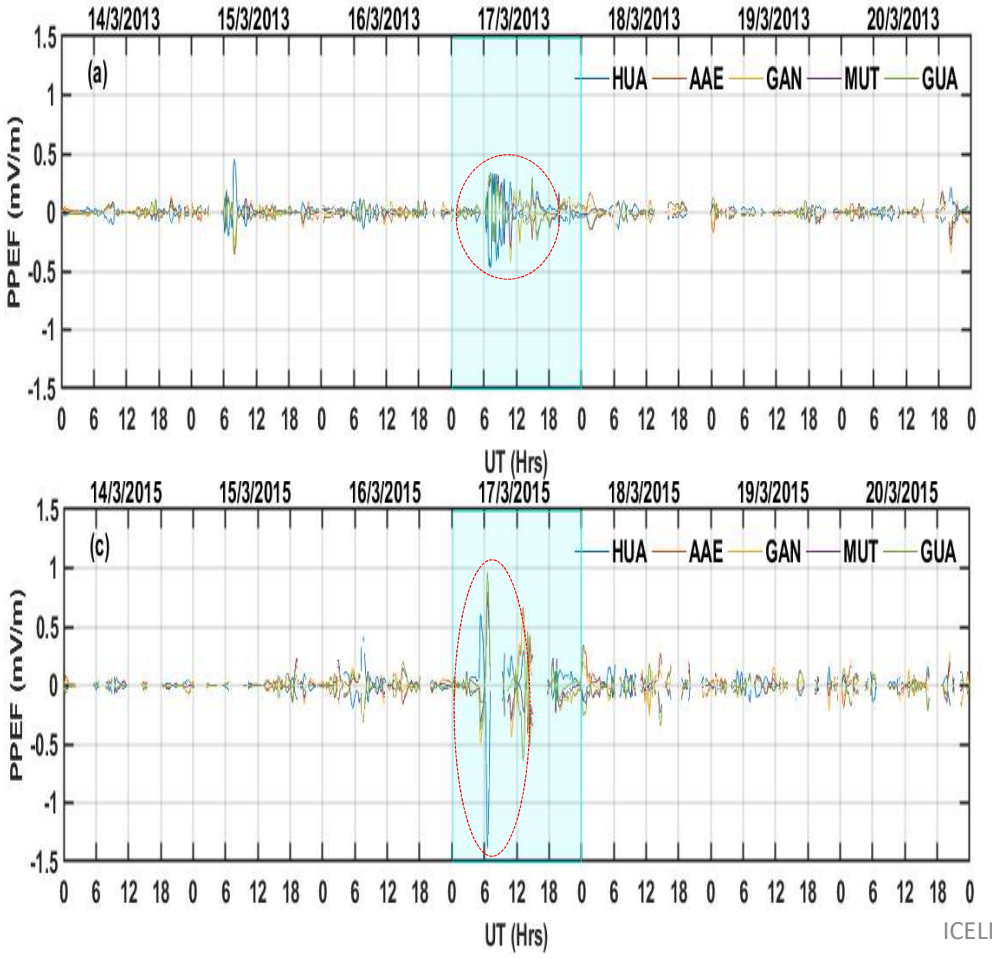

CIR G-Storms Model

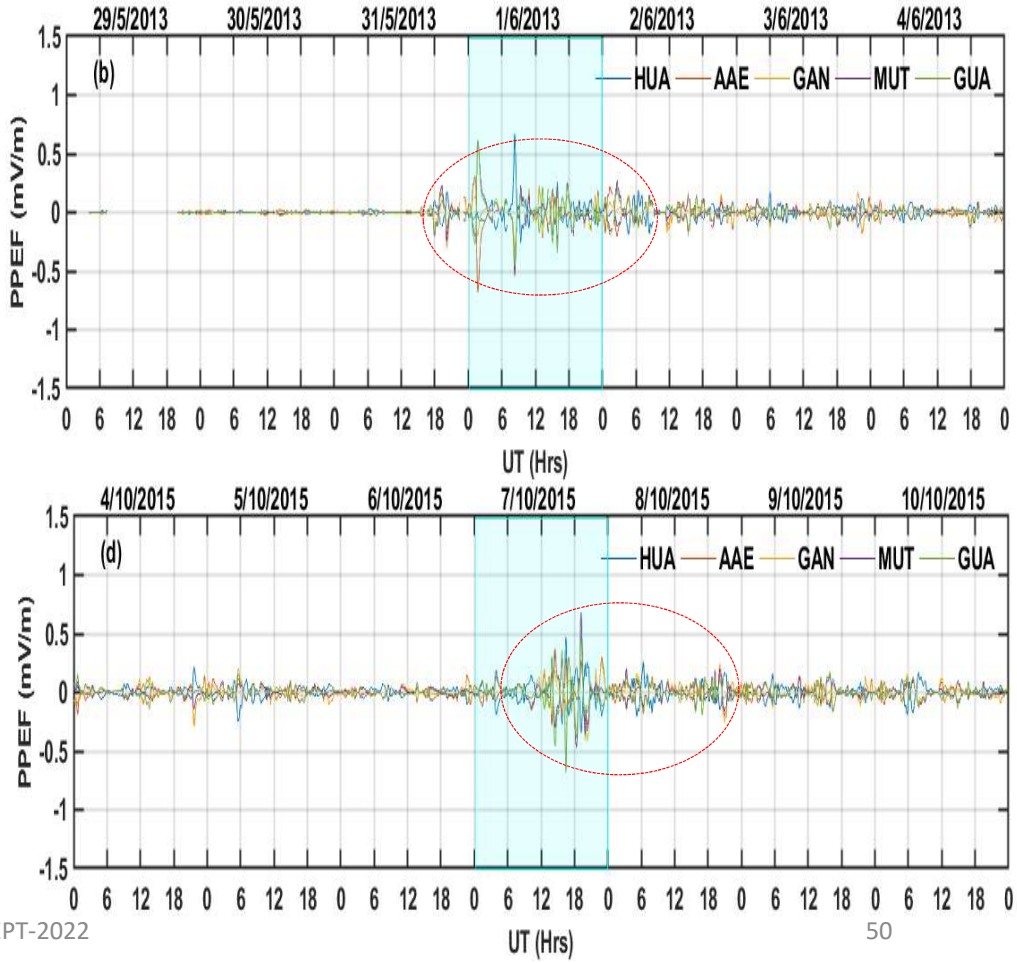

CME G-Storms

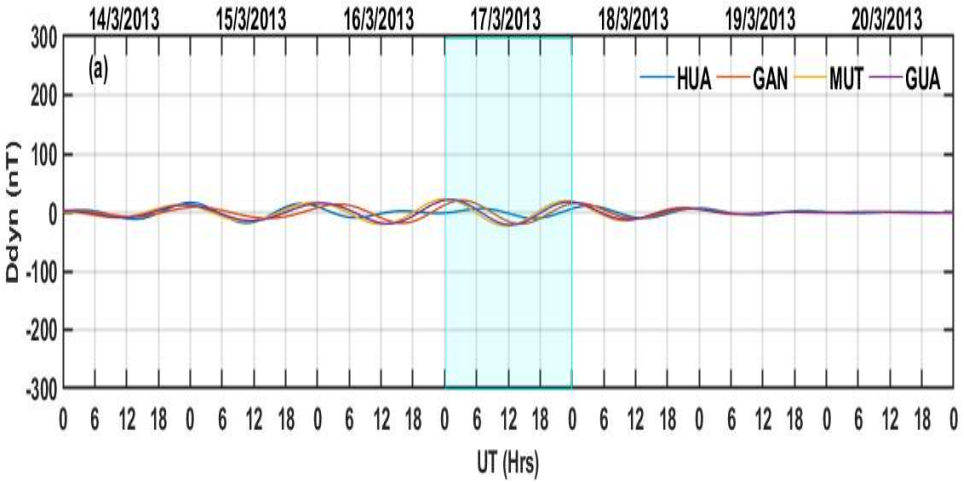

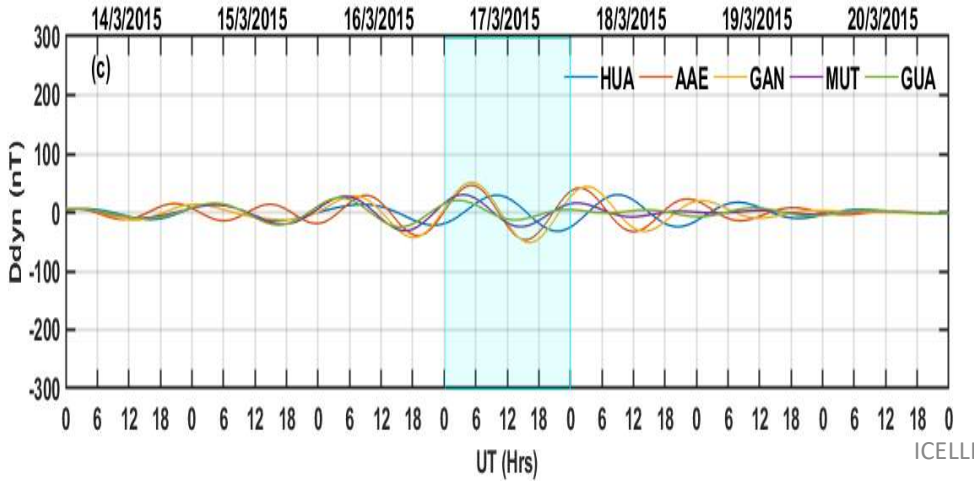

CIR G-Storms

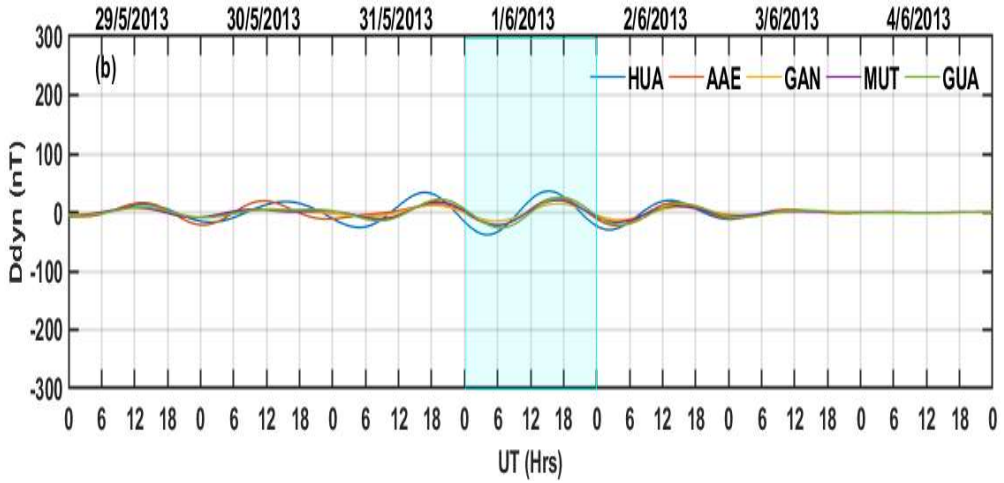

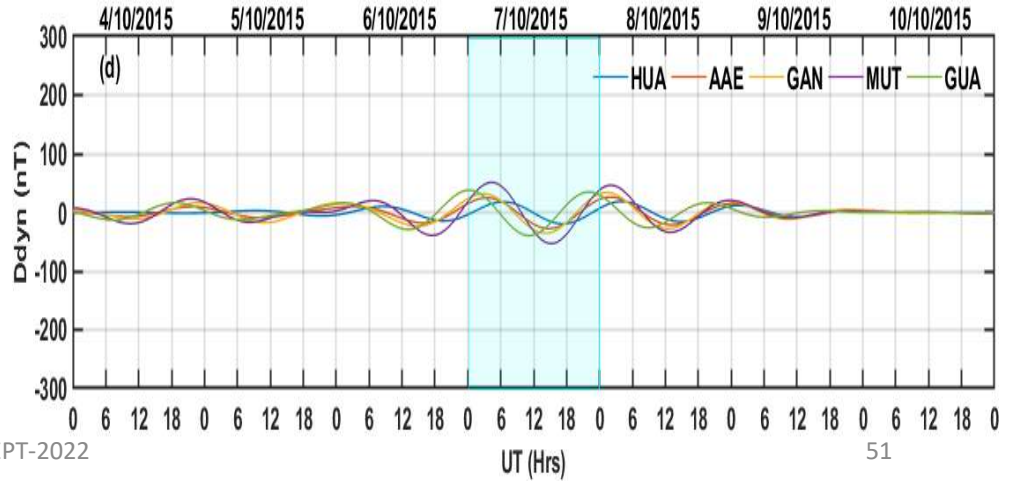

Summary 1/2

1. CIR-driven storms caused plasma density build-up at the interface of stream interaction regions to caused cause enhancements in plasma temperature and entropy, but this did not translate to enhancement in the geoeffectiveness of the resultant geomagnetic storms.

2. Despite the characteristic high-speed plasma of the CIR-driven storms, CME-driven storms still recorded higher ionospheric geoeffectiveness than CIR-driven storms. Geoeffectiveness of geomagnetic storms also followed semi-annual, with clear highest geoeffectiveness during March equinox and least during June solstice.

3. Aside from the seasonal effect above, the local time of storms' onset dictates ionospheric responses to geomagnetic storms, and this is the reason for the high TEC values obtained over the Indian Ocean/Asian sector as the local times of the storms' onset were around 1400 LT.

Summary 2/2

4. High occurrences of quiet-time irregularities were also observed in March 2013 and March 2015, and significantly high in the South American sector which we attributed to weak geomagnetic field configuration in the sector. Weak magnetic field flux density implies high vertical drift velocity ($E \times B/B^2$), which perhaps was the source of strength for the unusual plasma-upwelling in the evening-time F2-layer in the sector (Idolor et al., 2022).

5. A high O/N_2 ratio implies more recombination of ionospheric species, translating to higher ionospheric background plasma densities, while a lower O/N_2 ratio implies more dissociation of ionospheric species, translating to lower background plasma densities. This also explains why higher TEC was consistently recorded over the Indian Ocean/Asian sector.

Acknowledgments 1/2

Data: UNAVCO (http://www.unavco.org/data/data.html); SONEL (https://www.sonel.org/-GPS-.html?lang=en), IGS (https://cddis.nasa.gov/archive/gnss/data/daily/), World Data Center, Kyoto, Japan (http://wdc.kugi.kyoto-u.ac.jp/); Gopi Seemala for the TEC processing software, Cooperative Institute for Research in Environmental Sciences (CIRES), University of Colorado for PPEF model access: https://geomag.colorado.edu/real-time-model-of-the-ionosphericelectric-fields.html, GUVI O/N_2 data at http://guvitimed.jhuapl.edu/data_on2_info, SuperMag data at https://supermag.jhuapl.edu, NASA for the solar wind data and SYMH data at https://omniweb.gsfc.nasa.gov/ow_min.html.

Thank You for listening!

Adieu Pat Doherty!